

JAERI-Tech
2003-057



JP0350385



**EVALUATION OF NEUTRONIC CHARACTERISTICS OF
STACY 80-CM-DIAMETER CYLINDRICAL CORE FUELED
WITH 6% ENRICHED URANYL NITRATE SOLUTION**

June 2003

Hiroshi YANAGISAWA and Hiroki SONO

**日本原子力研究所
Japan Atomic Energy Research Institute**

本レポートは、日本原子力研究所が不定期に公刊している研究報告書です。

入手の問合わせは、日本原子力研究所研究情報部研究情報課（〒319-1195 茨城県那珂郡東海村）あて、お申し越してください。なお、このほかに財団法人原子力弘済会資料センター（〒319-1195 茨城県那珂郡東海村日本原子力研究所内）で複写による実費頒布をおこなっております。

This report is issued irregularly.

Inquiries about availability of the reports should be addressed to Research Information Division, Department of Intellectual Resources, Japan Atomic Energy Research Institute, Tokai-mura, Naka-gun, Ibaraki-ken, 319-1195, Japan.

© Japan Atomic Energy Research Institute, 2003

編集兼発行 日本原子力研究所

Evaluation of Neutronic Characteristics of STACY 80-cm-diameter Cylindrical Core Fueled with 6% Enriched Uranyl Nitrate Solution

Hiroshi YANAGISAWA and Hiroki SONO

**Department of Safety Research Technical Support
Nuclear Safety Research Center
Tokai Research Establishment
Japan Atomic Energy Research Institute
Tokai-mura, Naka-gun, Ibaraki-ken**

(Received April 24, 2003)

For the examination of neutronic safety design of forthcoming experimental core configurations in the Static Experiment Critical Facility (STACY), neutronic characteristics of 80-cm-diameter cylindrical cores fueled with 6% enriched uranyl nitrate solution have been evaluated by computational analyses. In the analyses, the latest nuclear data library, JENDL-3.3, was used as neutron cross section data. The neutron diffusion and transport calculations were performed using a diffusion code, CITATION, in the SRAC code system and a continuous-energy Monte Carlo code, MVP. Critical level heights of the cores were obtained using such parameters as uranium concentration (up to 500gU/l), free nitric acid concentration (up to 8mol/l), and concentration of soluble neutron poisons, gadolinium and boron. It has been confirmed from the evaluation that all critical cores comply with safety criteria required in the STACY operation concerning excess reactivity, reactivity addition rates and shutdown margins by safety rods.

Keywords: Neutronic Characteristics, Critical Experiment, STACY, 80-cm-diameter Cylindrical Core, 6% Enriched Uranyl Nitrate Solution, JENDL-3.3, Soluble Neutron Poison, Excess Reactivity, Reactivity Addition Rate, Shutdown Margin

6%濃縮硝酸ウラニル溶液を燃料としたSTACY 80cm直径円筒炉心の核特性評価

日本原子力研究所東海研究所安全性試験研究センター安全試験部

柳澤 宏司・曾野 浩樹

(2003年4月24日受理)

定常臨界実験装置(STACY)の次期実験炉心構成の核的安全設計を検討するために、6%濃縮硝酸ウラニル溶液を燃料とした80cm直径円筒炉心の核特性を計算によって評価した。本解析では、中性子断面積データとして最新の核データライブラリJENDL-3.3を使用した。SRACコードシステムの拡散コードCITATIONと連続エネルギーモンテカルロコードMVPを用いて中性子拡散及び輸送計算を行った。ウラン濃度(最大500gU/l)、遊離硝酸濃度(0~8mol/l)、ガドリニウム及びホウ素の可溶性中性子毒物の濃度をパラメータとして炉心の臨界液位を得た。評価の結果、全ての臨界炉心はSTACYの運転に要求される過剰反応度、反応度添加率、安全棒による停止余裕に関する安全基準に適合することが確認された。

Contents

1. Introduction	1
2. Core Configurations and Safety System	3
3. Calculation Method	6
4. Results and Discussion	10
4.1 Criticality Conditions	10
4.2 Excess Reactivity and Reactivity Addition Rate	18
4.3 Reactivity Effect by Free Surface Sloshing	19
4.4 Shutdown Margin by Safety Rods	20
5. Summary and Conclusion	27
Acknowledgement	27
References	27
Appendix-1 Reactivity Effects by Temperature Variation	30
Appendix-2 Validation of Calculation Method	32

目 次

1. はじめに	1
2. 炉心構成と安全系統	3
3. 計算方法	6
4. 結果と考察	10
4.1 臨界条件	10
4.2 過剰反応度と反応度添加率	18
4.3 自由液面の動揺による反応度効果	19
4.4 安全棒による停止余裕	20
5. まとめ	27
謝辞	27
参考文献	27
付録－1 温度変化による反応度効果	30
付録－2 計算方法の妥当性検証	32

List of Tables and Figures

Chap.2.		
Fig.2.1	80-cm-diameter cylindrical core tank, reproduced from Ref.1	4
Fig.2.2	Schematic diagram of STACY	5
Fig.2.3	Layout of electrodes in level meter	5
Chap.3.		
Fig.3.1	Models of CITATION calculation (R-Z cylindrical geometry)	7
Fig.3.2	Calculation procedures	7
Fig.3.3.1	Models of MVP calculation for sloshing effect	8
Fig.3.3.2	Models of MVP calculation for shutdown margins by safety rods for stationary surface	8
Fig.3.3.3	Models of MVP calculation for shutdown margins by safety rods for sloshing surface	9
Chap.4.		
Fig.4.1.1	Criticality conditions without soluble neutron poison	12
Fig.4.1.2	Criticality conditions with soluble neutron poisons: gadolinium	12
Fig.4.1.3	Criticality conditions with soluble neutron poison: boron	13
Fig.4.2	Typical differential reactivity of solution level height varying with critical level height (without soluble neutron poison; acidity: 0mol/l)	13
Fig.4.3.1	Differential reactivity of solution level height without soluble neutron poison	14
Fig.4.3.2	Differential reactivity of solution level height with soluble neutron poison: gadolinium	14
Fig.4.3.3	Differential reactivity of solution level height with soluble neutron poison: boron	15
Fig.4.4.1	Effective delayed neutron fraction without soluble neutron poison	15
Fig.4.4.2	Effective delayed neutron fraction with soluble neutron poison: gadolinium	16

Fig.4.4.3	Effective delayed neutron fraction with soluble neutron poison: boron	16
Fig.4.5.1	Prompt neutron lifetime without soluble neutron poison	17
Fig.4.5.2	Prompt neutron lifetime with soluble neutron poison: gadolinium	17
Fig.4.5.3	Prompt neutron lifetime with soluble neutron poison: boron	18
Fig.4.6	Reactivity effect caused by free surface sloshing	20
Fig.4.7.1(1)	Neutron multiplication factor in case of all safety rods inserted into solution without soluble neutron, having stationary surface	23
Fig.4.7.1(2)	Neutron multiplication factor in case of one safety rod not inserted into solution without soluble neutron poison, having stationary surface	23
Fig.4.7.2(1)	Neutron multiplication factor in case of all safety rods inserted into solution with soluble neutron poison: gadolinium, having stationary surface	24
Fig.4.7.2(2)	Neutron multiplication factor in case of one safety rod not inserted into solution with soluble neutron poison: gadolinium, having stationary surface	24
Fig.4.7.3(1)	Neutron multiplication factor in case of all safety rods inserted into solution with soluble neutron poison: boron, having stationary surface	25
Fig.4.7.3(2)	Neutron multiplication factor in case of one safety rod not inserted into solution with soluble neutron poison: boron, having stationary surface	25
Fig.4.8(1)	Neutron multiplication factor in case of all safety rods inserted into solution under sloshing condition (U conc. 500gU/l, Acidity 0mol/l)	26
Fig.4.8(2)	Neutron multiplication factor in case of one safety rod not inserted into solution under sloshing condition (U conc. 500gU/l, Acidity 0mol/l)	26
Appendix-1		
Fig.A.1.1	Reactivity effect by temperature variation of solution without soluble neutron poison	30
Fig.A.1.2	Reactivity effect by temperature variation of solution	

	with soluble neutron poison: gadolinium	31
Fig.A.1.3	Reactivity effect by temperature variation of solution	
	with soluble neutron poison: boron	31

Appendix-2

Table A.2.1	Results of benchmark tests on neutron multiplication factors of STACY 80-cm-diameter cylindrical cores fueled with 10% enriched uranyl nitrate solution	32
Table A.2.2	Comparisons of differential reactivity of solution level height between CITATION and TWOTRAN codes on STACY 80-cm-diameter cylindrical cores fueled with 6% enriched uranyl nitrate solution (U conc. 500gU/l, acidity 0mol/l, without soluble neutron poisons)	33
Table A.2.3	Results of benchmark tests on neutron multiplication factors of uranyl nitrate solution systems (70gU/l) containing gadolinium	35
Table A.2.4	Results of benchmark tests on neutron multiplication factors of uranyl nitrate solution systems containing boron carbide absorber rods	38
Table A.2.5	Results of benchmark tests on kinetic parameters (β_{eff}/ℓ) of STACY 80-cm-diameter cylindrical cores fueled with 10% enriched uranyl nitrate solution	39
Figure A.2.1	Ratio of calculated neutron multiplication factor	35
Figure A.2.2	Neutron energy spectra of IPPE Case 1 experiment using uranyl nitrate solution (70gU/l) containing gadolinium	36
Figure A.2.3	Neutron energy spectra of IPPE Case 3 experiment using uranyl nitrate solution (70gU/l) containing gadolinium	37

図表リスト

2章

Fig.2.1	80cm 直径円筒型炉心タンク, 参考文献1より	4
Fig.2.2	STACY 構成の概要	5
Fig.2.3	液位計電極の配置	5

3章

Fig.3.1	CITATION 計算モデル (R-Z 円筒体系)	7
Fig.3.2	計算手続き	7
Fig.3.3.1	液面動揺効果の MVP 計算モデル	8
Fig.3.3.2	静止液面の安全棒による停止余裕の MVP 計算モデル	8
Fig.3.3.3	動揺液面の安全棒による停止余裕の MVP 計算モデル	9

4章

Fig.4.1.1	可溶性中性子毒物なしでの臨界条件	12
Fig.4.1.2	可溶性中性子毒物:ガドリニウムありでの臨界条件	12
Fig.4.1.3	可溶性中性子毒物:ホウ素ありでの臨界条件	13
Fig.4.2	臨界液位の変化に対する微分液位反応度の典型 (可溶性中性子毒物なし,酸濃度 0mol/l)	13
Fig.4.3.1	可溶性中性子毒物なしでの微分液位反応度	14
Fig.4.3.2	可溶性中性子毒物:ガドリニウムありでの微分液位反応度	14
Fig.4.3.3	可溶性中性子毒物:ホウ素ありでの微分液位反応度	15
Fig.4.4.1	可溶性中性子毒物なしでの実効遅発中性子割合	15
Fig.4.4.2	可溶性中性子毒物:ガドリニウムありでの 実効遅発中性子割合	16
Fig.4.4.3	可溶性中性子毒物:ホウ素ありでの実効遅発中性子割合	16
Fig.4.5.1	可溶性中性子毒物なしでの即発中性子寿命	17
Fig.4.5.2	可溶性中性子毒物:ガドリニウムありでの即発中性子寿命	17
Fig.4.5.3	可溶性中性子毒物:ホウ素ありでの即発中性子寿命	18
Fig.4.6	自由液面動揺による反応度効果	20
Fig.4.7.1(1)	静止液面を有する可溶性中性子毒物を含まない溶液への 安全棒全数挿入時の中性子実効増倍率	23
Fig.4.7.1(2)	静止液面を有する可溶性中性子毒物を含まない溶液への	

	安全棒1本が挿入不能時の中性子実効増倍率	23
Fig.4.7.2(1)	静止液面を有する可溶性中性子毒物:ガドリニウムを含む 溶液への安全棒全数挿入時の中性子実効増倍率	24
Fig.4.7.2(2)	静止液面を有する可溶性中性子毒物:ガドリニウムを含む 溶液への安全棒1本が挿入不能時の 中性子実効増倍率	24
Fig.4.7.3(1)	静止液面を有する可溶性中性子毒物:ホウ素を含む 溶液への安全棒全数挿入時の中性子実効増倍率	25
Fig.4.7.3(2)	静止液面を有する可溶性中性子毒物:ホウ素を含む 溶液への安全棒1本が挿入不能時の 中性子実効増倍率	25
Fig.4.8(1)	動揺液面における安全棒全数挿入時の中性子実効増倍率 (U 濃度 500gU/l, 酸濃度 0mol/l)	26
Fig.4.8(2)	動揺液面における安全棒1本が挿入不能時の 中性子実効増倍率 (U 濃度 500gU/l, 酸濃度 0mol/l)	26
付録ー1		
Fig.A.1.1	可溶性中性子毒物を含まない溶液の温度変化による 反応度効果	30
Fig.A.1.2	可溶性中性子毒物:ガドリニウムを含む溶液の温度変化による 反応度効果	31
Fig.A.1.3	可溶性中性子毒物:ホウ素を含む溶液の温度変化による 反応度効果	31
付録ー2		
Table A.2.1	10%濃縮硝酸ウラニル溶液による STACY 80cm 直径 円筒炉心の中性子実効増倍率に関する ベンチマークテスト結果	32
Table A.2.2	6%濃縮硝酸ウラニル溶液による STACY 80cm 直径 円筒炉心の中性子実効増倍率に関する CITATION コードと TWOTRAN コードによる 微分液位反応度の比較(ウラン濃度 500gU/l, 酸濃度 0mol/l, 可溶性中性子毒物なし)	33
Table A.2.3	ガドリニウムを含む硝酸ウラニル溶液体系 (70gU/l) の 中性子実効増倍率に関する	

ベンチマークテスト結果	35
Table A.2.4 炭化ホウ素中性子吸収棒を含む硝酸ウラニル溶液体系の 中性子実効増倍率に関するベンチマークテスト結果	38
Table A.2.5 10%濃縮硝酸ウラニル溶液による STACY 80cm 直径 円筒炉心の動特性パラメータ(β_{eff}/ℓ)に関する ベンチマークテスト結果	39
Figure A.2.1 計算された中性子実効増倍率の比	35
Figure A.2.2 ガドリニウムを含む硝酸ウラニル溶液(70gU/l)を用いた IPPE ケース1実験の中性子エネルギースペクトル	36
Figure A.2.3 ガドリニウムを含む硝酸ウラニル溶液(70gU/l)を用いた IPPE ケース3実験の中性子エネルギースペクトル	37

This is a blank page.

1. Introduction

For the purpose of nuclear criticality safety of spent fuel reprocessing plants, the Japan Atomic Energy Research Institute (JAERI) has performed critical experiments since 1995 using a solution-fueled critical facility, named STACY¹⁾ (Static Experiment Critical Facility). In STACY, 10% enriched uranyl nitrate solution had been utilized for various homogeneous core configurations since the first criticality. A series of STACY experiments provided basic criticality data under reflected and unreflected conditions, kinetic parameters, *i.e.* ratios of effective delayed neutron fraction to prompt neutron lifetime, and so on.²⁻⁶⁾ The experiments with 10% enriched uranyl nitrate solution had been completed in 2001.

Following those experiments, heterogeneous core configurations¹⁾ have been tested in STACY since 2002 using 6% enriched uranyl nitrate solution and 5% enriched uranium dioxide fuel pins to simulate systems containing fissile materials in solution and solid forms as models of a spent fuel dissolver. The experiments on the heterogeneous configurations are currently planned for 3 years in total, as varying square pitches of a fuel pin lattice. The reactivity effect brought by soluble neutron poisons in the solution will be measured in the final year.

Prior to the heterogeneous experiments with soluble neutron poisons, experiments on homogeneous cores with an 80-cm-diameter cylindrical tank^{1,3,4,6)} are also scheduled in 2004 using 6% enriched uranyl nitrate solution. These experiments are considered to be important and indispensable because they will provide comparative data on criticality characteristics and biases of computation between 10% and 6% enriched uranium solution systems. Also, the differences in the characteristics and biases between homogeneous and heterogeneous systems will be easily confirmed due to the same enrichment of the uranium solution.

As preparation for the experiments on the 80-cm-diameter cylindrical cores fueled with 6% enriched uranyl nitrate solution, the examination of neutronic design has been performed by computational analyses from the safety point of view. In STACY, all critical cores must comply with safety criteria on excess reactivity, reactivity addition rates at the vicinity of a critical level height, and shutdown margins by safety rods.¹⁾ They are represented as 'neutronic limitations' and fundamental safety criteria for STACY operations. In general, the compliance with these criteria has to be confirmed at design and operation stages according to the Japanese regulations for

nuclear reactors. At the design stage, the confirmation is normally made by computational analyses, and then completed at the next stage using operational and experimental data as well as computation. The present examination corresponds to the former stage.

For this purpose, critical level heights of 80-cm-diameter cylindrical cores fueled with 6%-enriched uranyl nitrate solution in STACY were surveyed by using a neutron diffusion code with such parameters as uranium concentration, concentration of free nitric acid, concentration of soluble neutron poisons, gadolinium and boron. The compliance with the safety criteria for all critical cores was confirmed using a continuous-energy Monte Carlo code as well as the diffusion code.

In Chap.2, core configurations are presented briefly. The procedures of calculations are described in Chap.3. Results of the analyses and discussion are summarized in Chap.4. In Chap.5, the present work is concluded.

2. Core Configurations and Safety System

Details of the configuration of an 80-cm-diameter cylindrical core system were presented in an earlier report.¹⁾ Figure 2.1 shows an 80-cm-diameter cylindrical core tank. The solution core is composed by feeding uranyl nitrate solution into the core tank made of stainless steel. Uranium concentration of the solution is limited up to 500gU/l. Critical level heights are also limited from 40 to 140cm. The reactivity is controlled by the solution level height in the core tank, which is changed by feed of the solution by a pump. No control rod is utilized for the operation.

The schematic diagram of STACY is illustrated in Fig.2.2. STACY is equipped with two sorts of solution feed systems, the fast and slow pumps. The slow pump (0.7 to 10 l/min) is utilized for reactivity control at the vicinity of a critical level height. The incremental speed of a level height is limited up to 0.5mm/s by the slow pump. Devices for driving safety rods and a level meter are installed on the top of the core tank.¹⁾ The safety rod, boron carbide pellets in a stainless steel pipe, is used for only emergency shutdown. For the 80-cm-diameter cylindrical core tank, 6 safety rods are installed and inserted automatically into the solution in case of emergency. The level meter controls excess reactivity represented by a solution level height beyond criticality. The level meter is equipped with electrodes, which detect a solution surface.

Figure 2.3 shows the layout of the electrodes. At the vicinity of a critical level height, a lower electrode is positioned manually at a lower level than that corresponding to 0.17\$ of excess reactivity. The lower electrode functions as stoppage of the solution feed when the solution surface reaches there. Two higher electrodes are fixed at the level being 1.8mm higher than the lower electrode. The higher electrodes are backup systems and used for emergency shutdown in case of malfunctions of the lower electrode. In STACY, the maximum excess reactivity is defined as the reactivity corresponding to the level of the higher electrodes, considering hypothetical loss of the function of the lower electrode.

STACY has three sorts of safety criteria in terms of neutronic limitations, as follows,

- 1) Maximum excess reactivity must be within 0.8\$,
- 2) Reactivity addition rates by the slow pump at the vicinity of a critical level height must be within 3cent/s,
- 3) Regarding shutdown margins by safety rods, neutron multiplication factors must

be within 0.985 in the case of all safety rods inserted into the solution, and 0.995 in the case of one safety rod not inserted hypothetically due to its malfunction. For the maximum excess reactivity and reactivity addition rates, the differential reactivity²⁾ of solution level height is an important parameter as neutronic characteristics of cores since they depend greatly upon the reactivity variation due to increase of the level height.

As the other important neutronic characteristics particularly for solution cores, reactivity effects by sloshing^{7,8)} of a free solution surface brought by an earthquake should be taken into account. In STACY, the reactivity added by the surface sloshing has to be negative for all critical core configurations.

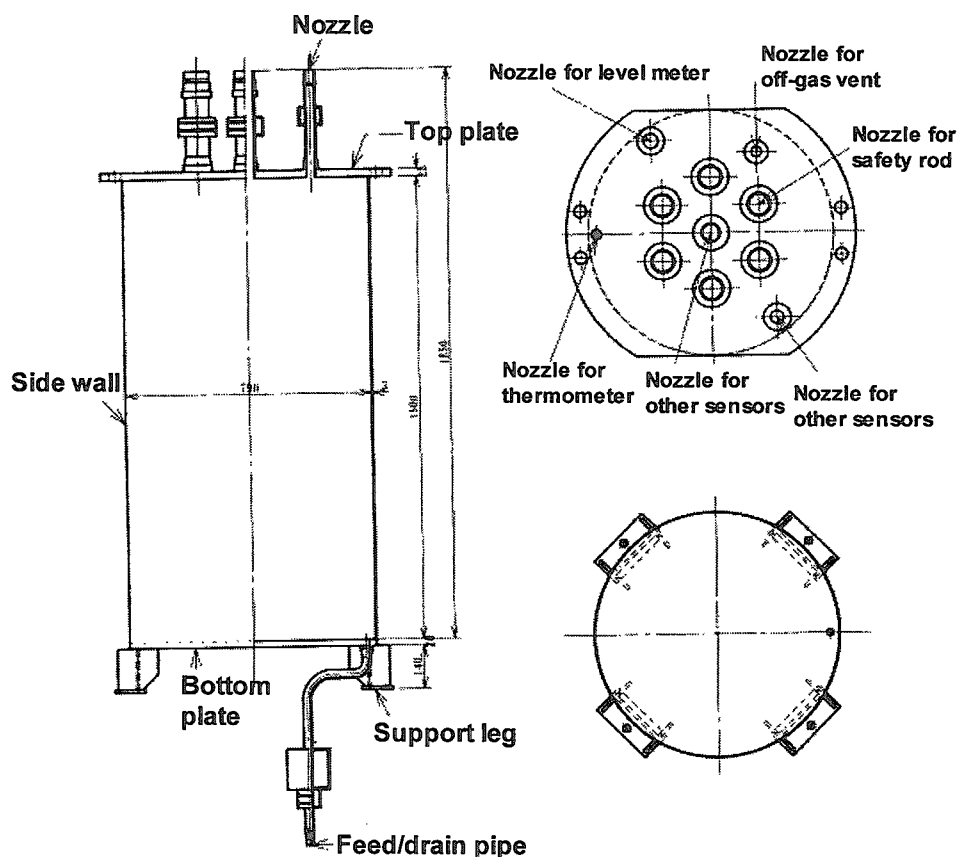


Figure 2.1 80-cm-diameter cylindrical core tank, reproduced from Ref.1

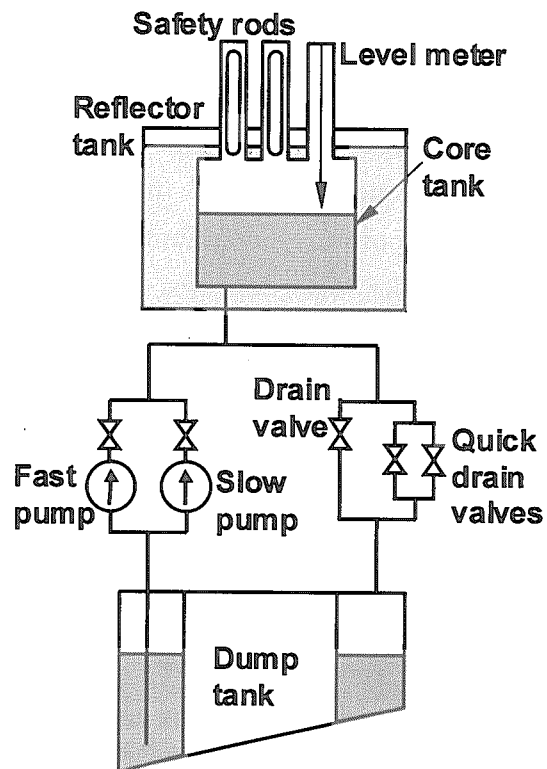


Figure 2.2 Schematic diagram of STACY

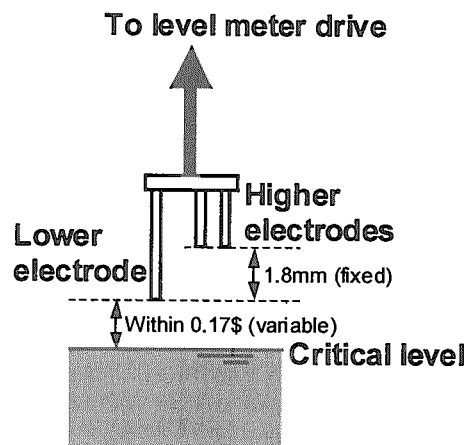


Figure 2.3 Layout of electrodes in level meter

3. Calculation Method

Critical level heights were surveyed by using a neutron diffusion code, CITATION,⁹⁾ in the SRAC¹⁰⁾ code system, with such parameters as uranium concentration (up to 500gU/l), concentration of free nitric acid (up to 8mol/l), concentration of soluble neutron poison (gadolinium and boron). Two-dimensional cylindrical models were used under water-reflected and unreflected conditions, as shown in Fig.3.1. Procedures of the calculation are illustrated in Fig.3.2. The Japanese Evaluated Nuclear Data Library, JENDL-3.3,¹¹⁾ was used as cross section data. Atomic number densities of the solution were obtained by the density equation reported by Sakurai *et al.*¹²⁾ The atomic number densities of stainless steel and water were cited from Ref.3. Temperature of all materials was set to be 25°C. Temperature effects are shown in the Appendix-1. For critical core configurations, the differential reactivity of solution level height (dp/dh), effective delayed neutron fraction (β_{eff}), and prompt neutron lifetime (ℓ) were also calculated by the CITATION code.

For the calculations of surface sloshing effects and shutdown margins by safety rods, a continuous-energy Monte Carlo code, MVP,^{13,14)} was used. Figures 3.3.1, 3.3.2 and 3.3.3 show calculation models. In the case of sloshing effects, the solution surface brought by the first-degree-spatial mode was taken into account, which had been found to be the dominant mode from mock-up tests performed by using the Large-Scale Earthquake Simulator at the National Research Institute for Earth Science and Disaster Prevention, Japan.¹⁵⁾ In the mock-up tests, the design basis earthquake, S_1 ¹⁶⁾ (334cm/s² of peak acceleration on the floor of STACY reactor room), had been taken into account. The shutdown margins by safety rods were calculated under the sloshing conditions as well as stationary ones. The maximum level variation (ΔH_s) under the sloshing conditions was considered conservatively up to 30cm although the mock-up tests had shown 25cm of ΔH_s in maximum. The cross section library, atomic number densities and temperature of materials were the same as those in the CITATION calculations. The density of natural-boron carbide of safety rods was 2.38g/cm³. The number of particle histories was 5 millions (25,000 particles per batch by 300 batches, initial 100 batches skipped) for all cases. The validity of the calculation methods is discussed in the Appendix-2.

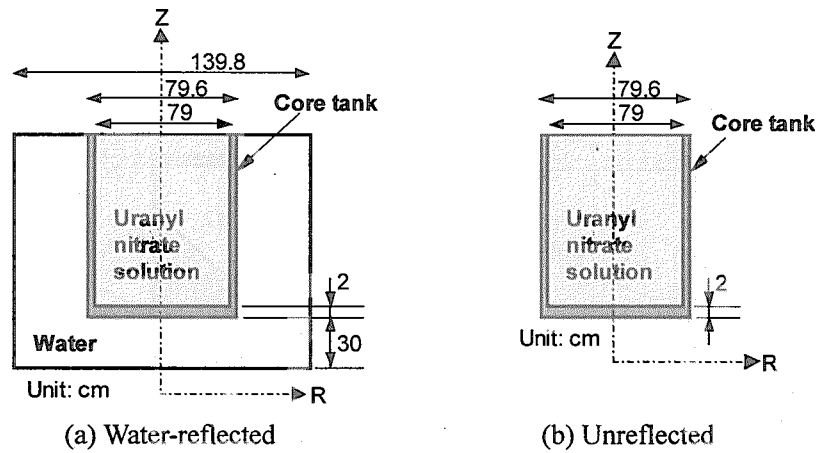


Figure 3.1 Models of CITATION calculation (R-Z cylindrical geometry)

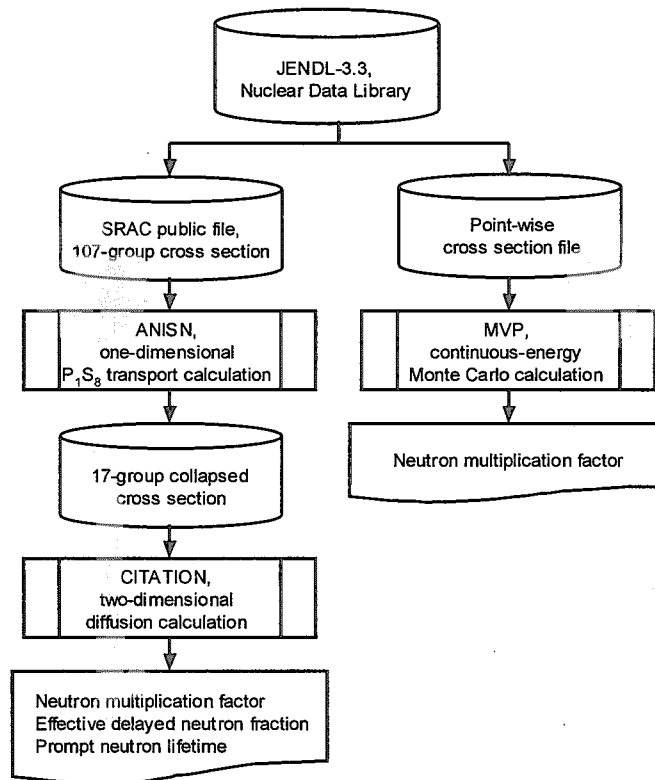


Figure 3.2 Calculation procedures

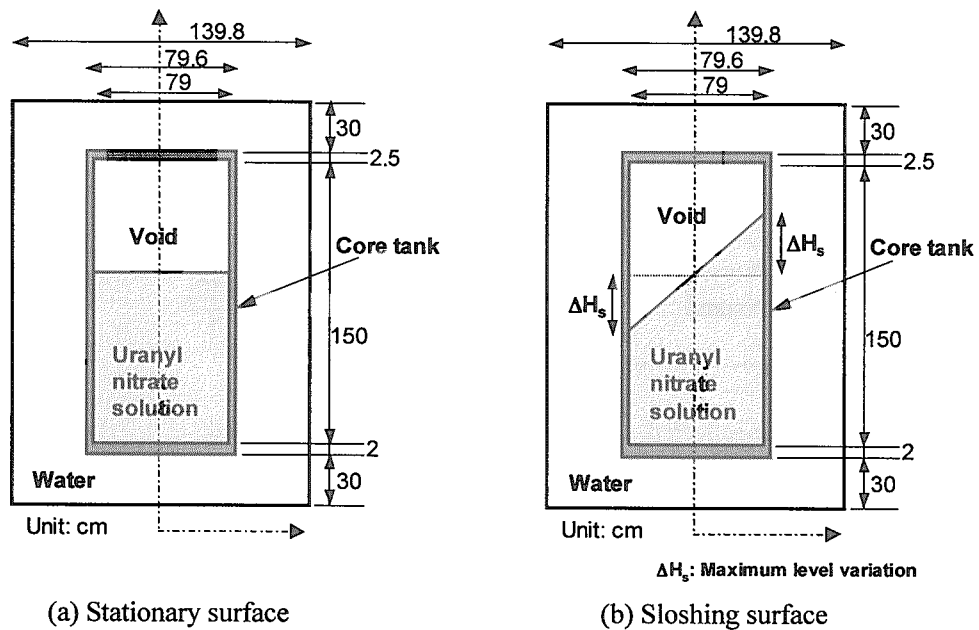


Figure 3.3.1 Models of MVP calculation for sloshing effect
The water is replaced by void in case of unreflected conditions.

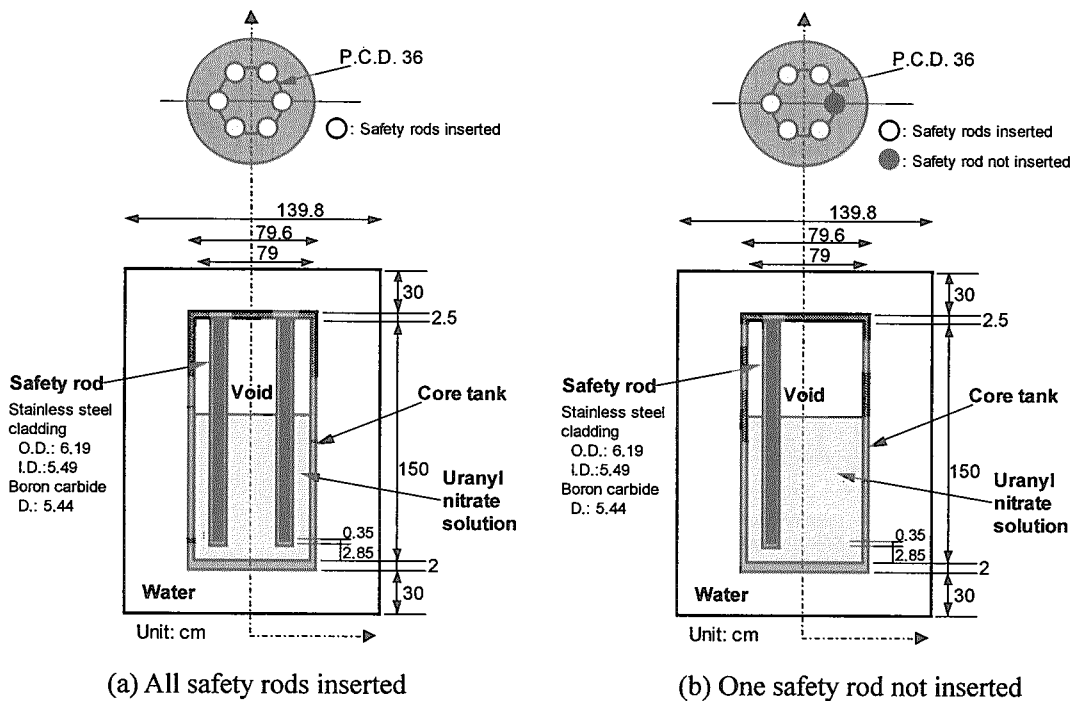
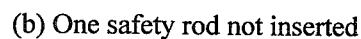


Figure 3.3.2 Models of MVP calculation for shutdown margins by safety rods for stationary surface
The water is replaced by void in case of unreflected conditions.



The water is replaced by void in case of unreflected conditions.

4. Results and Discussion

4.1 Criticality Conditions

Figure 4.1.1 shows the relation between critical level heights and uranium concentration for cores not containing soluble neutron poisons. The critical level height decreases monotonously as the uranium concentration increases. In the case of 0mol/l of free nitric acid concentration, the uranium concentration can be changed from 330 to 500gU/l under the water-reflected conditions. As the free nitric acid concentration increases, the range of the uranium concentration for the attainment of criticality becomes smaller because of neutron absorption by ^{14}N in nitric acid. The relations between critical level heights and concentration of gadolinium and boron are shown in Figs. 4.1.2 and 4.1.3, respectively, under the conditions of 400 and 500gU/l of uranium concentration. It is found that the maximum concentration of gadolinium and boron are 0.068 gGd/l and 0.23gB/l, respectively.

The differential reactivity of solution level height ($d\rho/dh$) varies mainly with the critical level height.²⁾ According to the well-known modified one-group diffusion theory, it can be expressed by,

$$\frac{d\rho}{dh} = \frac{C}{(H_c + \lambda)^3}, \dots\dots\dots (4.1.1)$$

where H_c , λ and C represent a critical level height, an extrapolated distance and a constant, respectively. Figure 4.2 shows a typical tendency of the differential reactivity of solution level height against the critical level height. The reactivity is represented in the unit of \$ by using the calculated effective delayed neutron fractions described below. The differential reactivity of solution level height becomes the maximum at the minimum critical level height (40cm), as foreseen by Eq.(4.1.1). The variations of the differential reactivity of solution level height with the uranium concentration and the concentration of soluble neutron poisons are also shown in Figs. 4.3.1, 4.3.2 and 4.3.3, respectively. The differential reactivity of solution level height increases as the uranium concentration increases and the concentration of soluble neutron poison decreases because these variations of the concentration lead to lower critical level heights. The maximum differential reactivity of solution level height, 0.072\$/mm, is confirmed under the following

condition.

- Uranium concentration: 500gU/ ℓ .
- Concentration of free nitric acid: 0mol/ ℓ .
- Soluble neutron poison: none.
- Critical level height: 40.0cm.
- Reflector: water.

Figures 4.4.1, 4.4.2 and 4.4.3 show the effective delayed neutron fraction (β_{eff}). The effective delayed neutron fraction increases as the uranium concentration increases and the concentration of soluble neutron poisons decreases. This is because these variations of the concentration lead to lower critical level height and to larger leakage of neutron from the core. The effective delayed neutron fraction under unreflected conditions is found to be slightly larger than that under water-reflected conditions because the neutron leakage of unreflected systems is larger than that of reflected systems.

Also, Figs 4.5.1, 4.5.2 and 4.5.3 show the prompt neutron lifetime (ℓ). The prompt neutron lifetime decreases as the uranium concentration and concentration of soluble neutron poison increases. This is because these variations of the concentration lead to larger absorption of neutron in the core. The prompt neutron lifetime under unreflected conditions is found to be slightly smaller than that under water-reflected conditions because the neutron leakage of unreflected systems is larger than that of reflected systems.

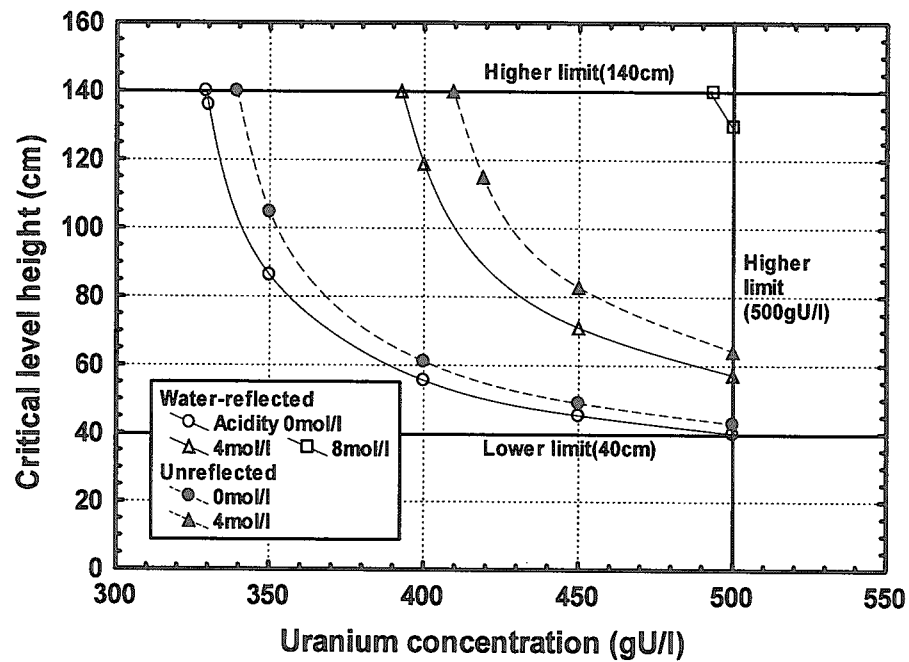


Figure 4.1.1 Criticality conditions without soluble neutron poison

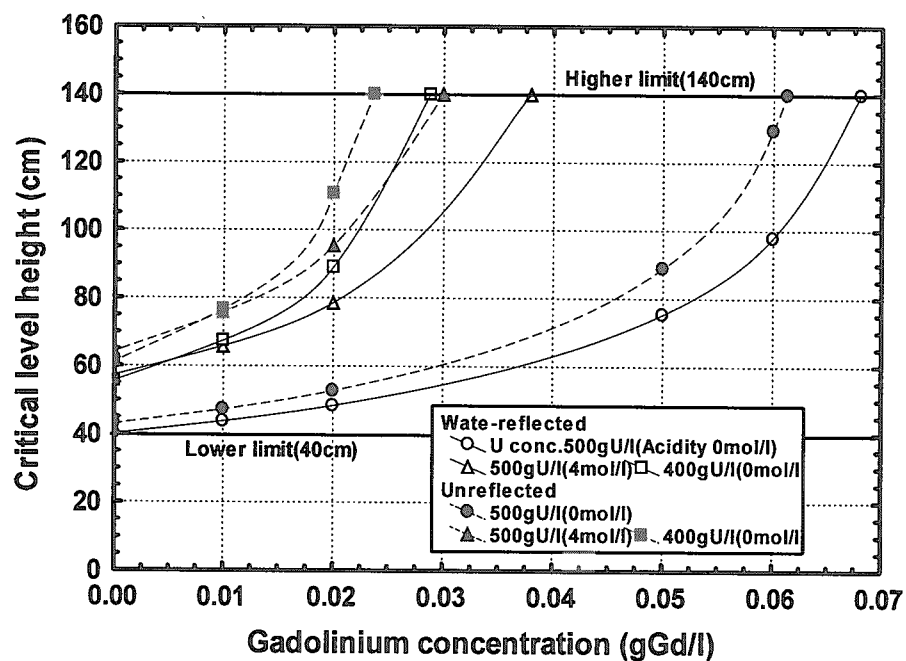


Figure 4.1.2 Criticality conditions with soluble neutron poisons: gadolinium

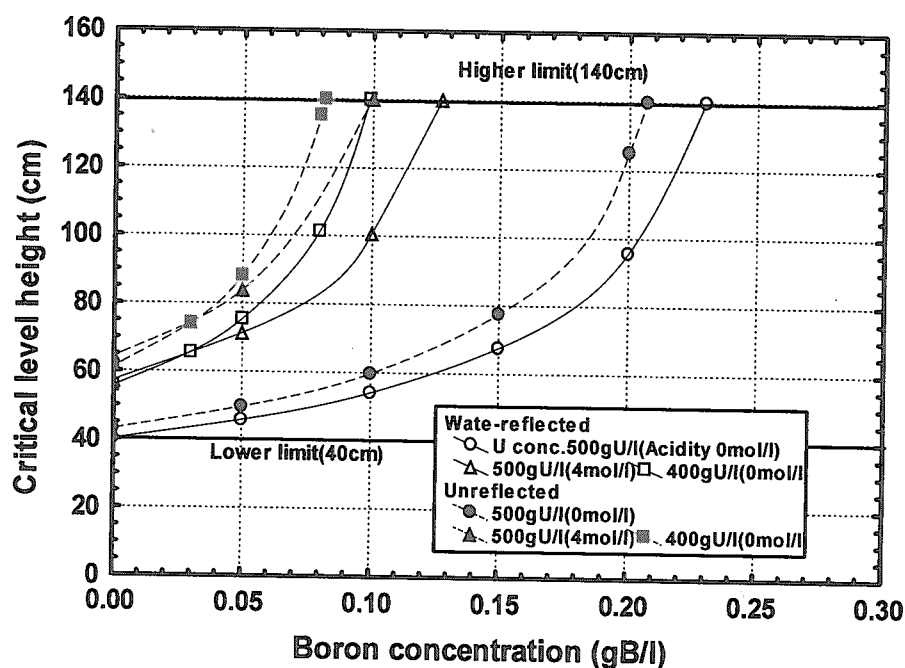


Figure 4.1.3 Criticality conditions with soluble neutron poison: boron

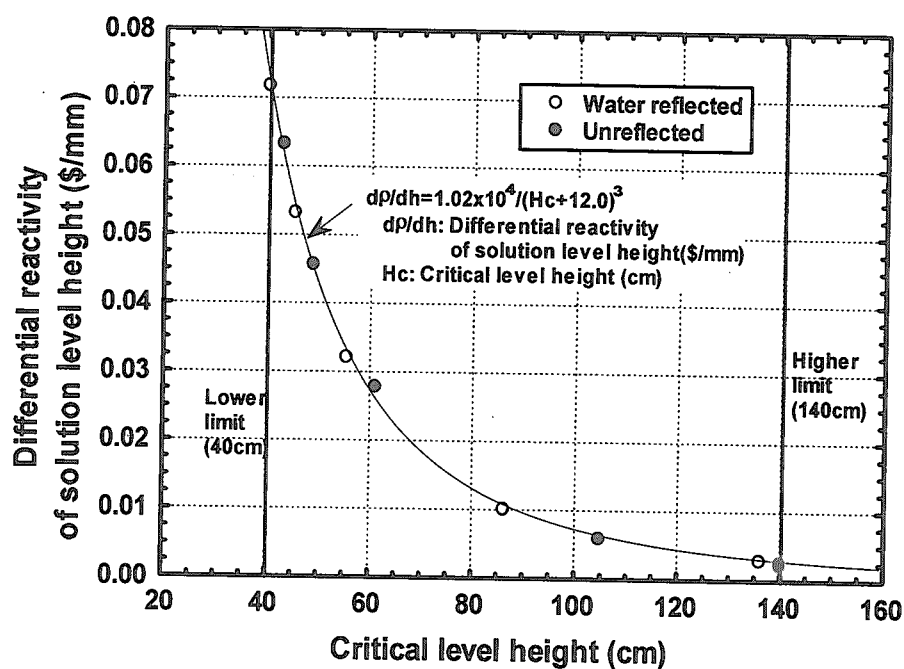


Figure 4.2 Typical differential reactivity of solution level height varying with critical level height (without soluble neutron poison; acidity: 0mol/l)

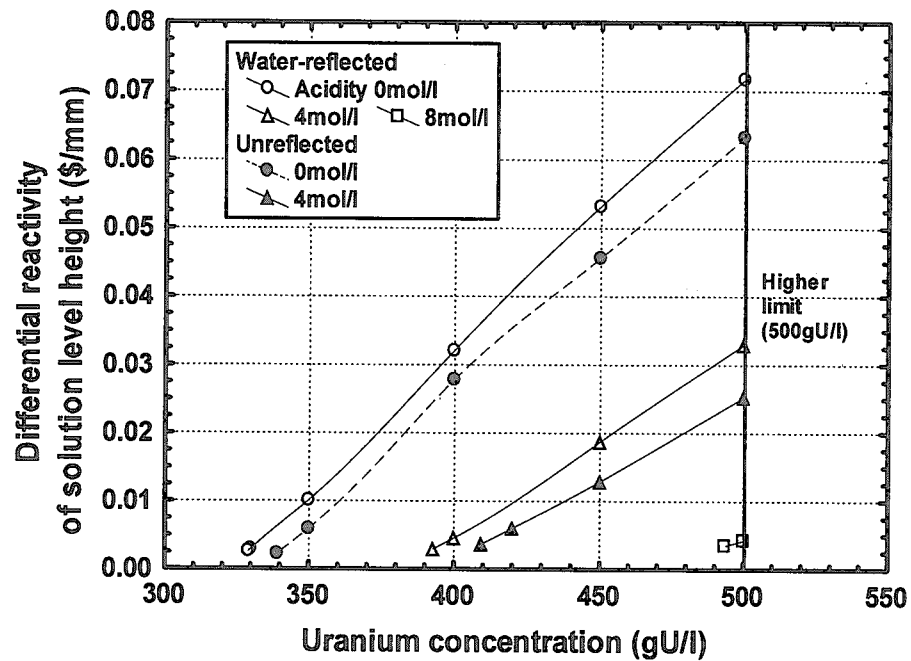


Figure 4.3.1 Differential reactivity of solution level height without soluble neutron poison

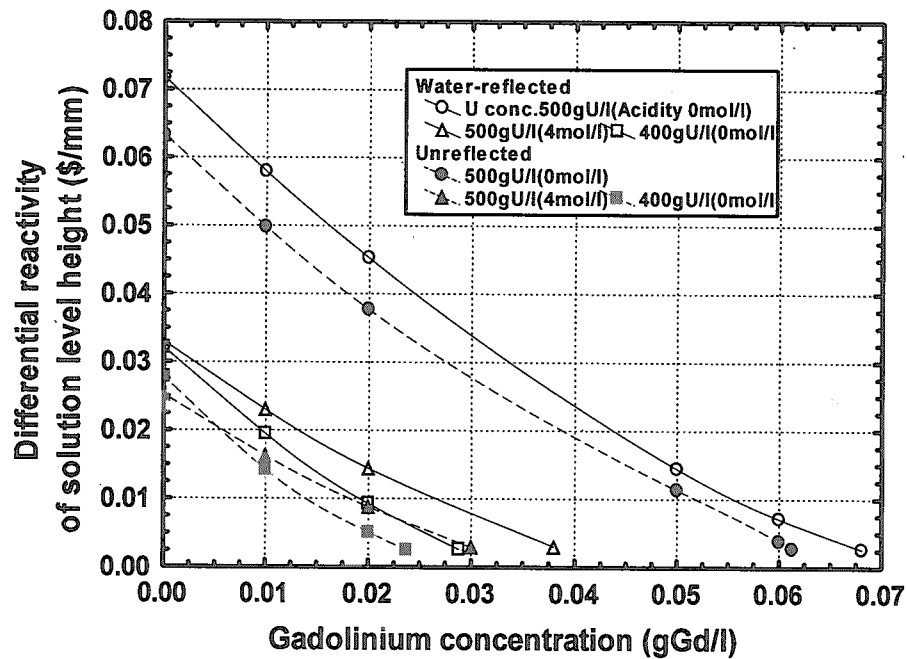


Figure 4.3.2 Differential reactivity of solution level height with soluble neutron poison: gadolinium

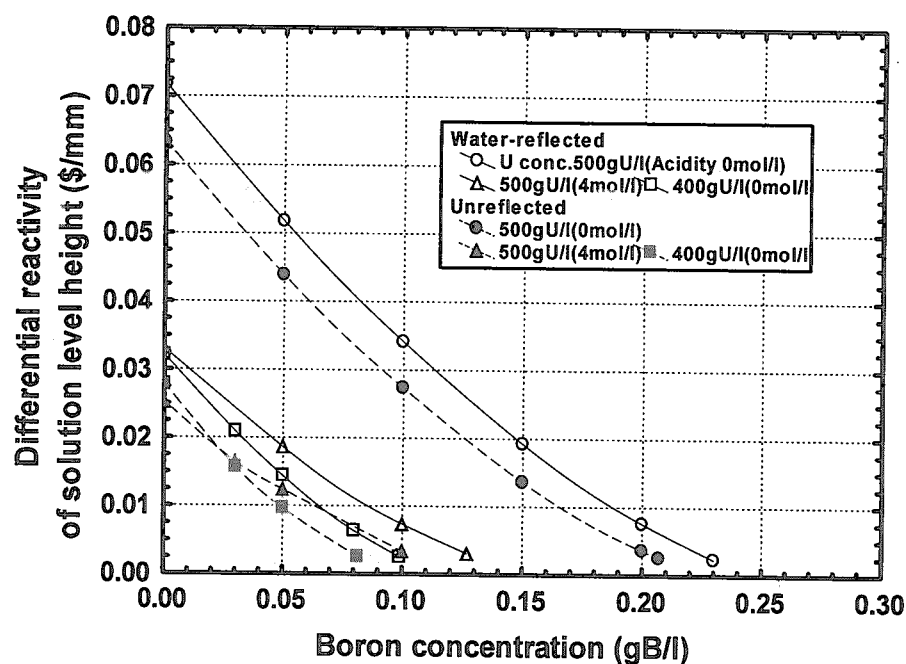


Figure 4.3.3 Differential reactivity of solution level height with soluble neutron poison: boron

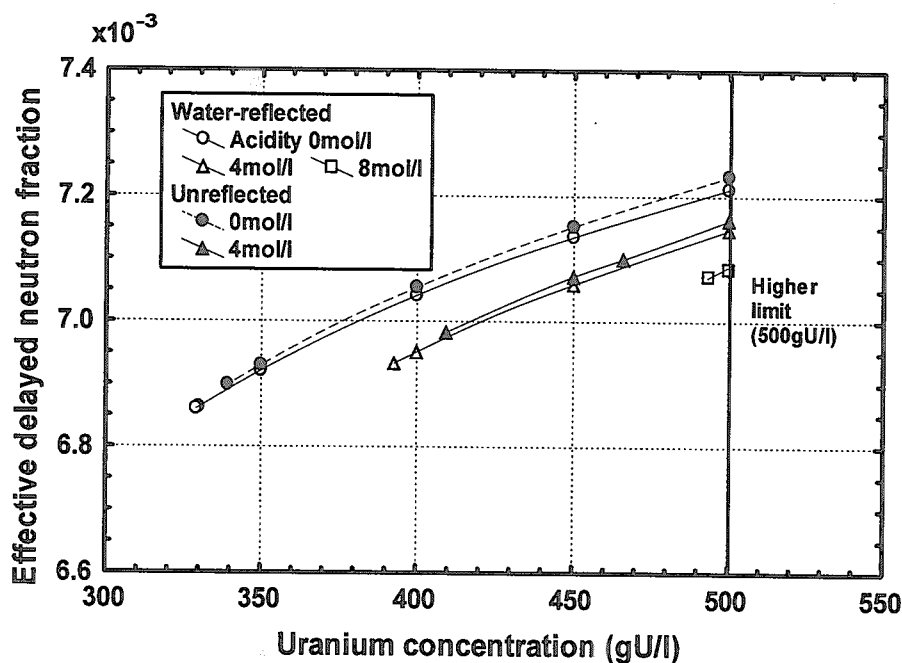


Figure 4.4.1 Effective delayed neutron fraction without soluble neutron poison

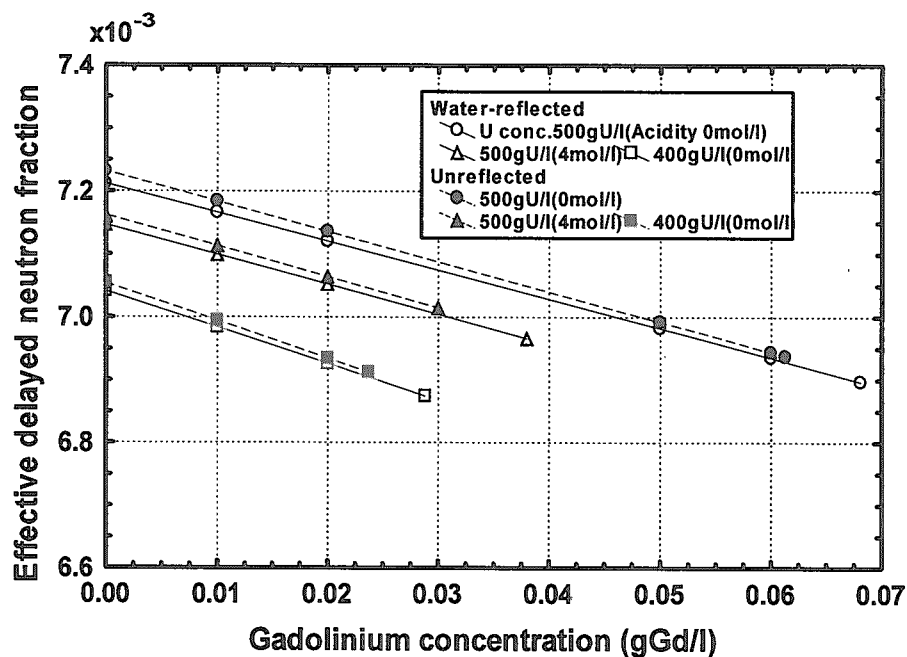


Figure 4.4.2 Effective delayed neutron fraction with soluble neutron poison: gadolinium

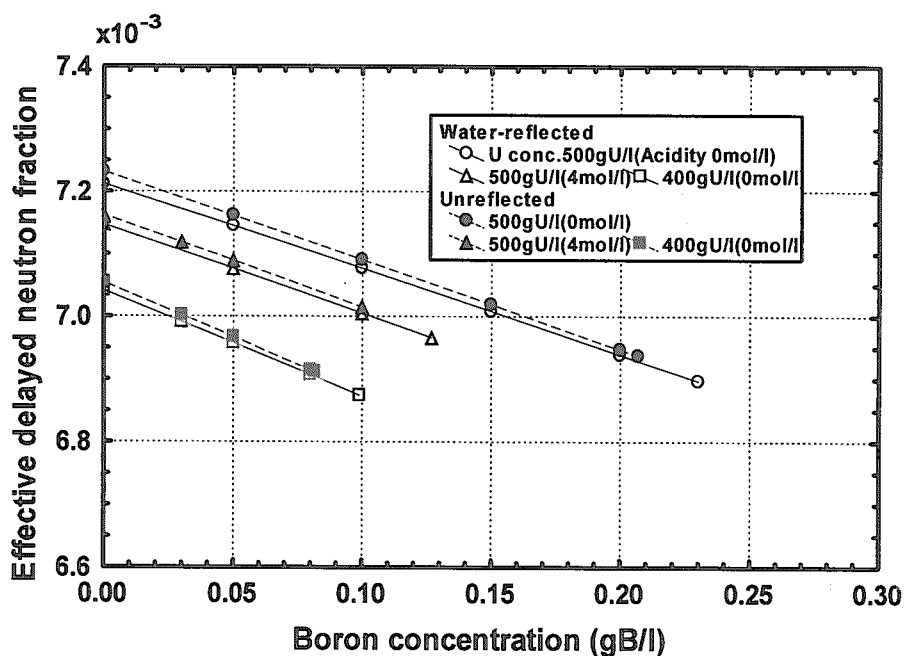


Figure 4.4.3 Effective delayed neutron fraction with soluble neutron poison: boron

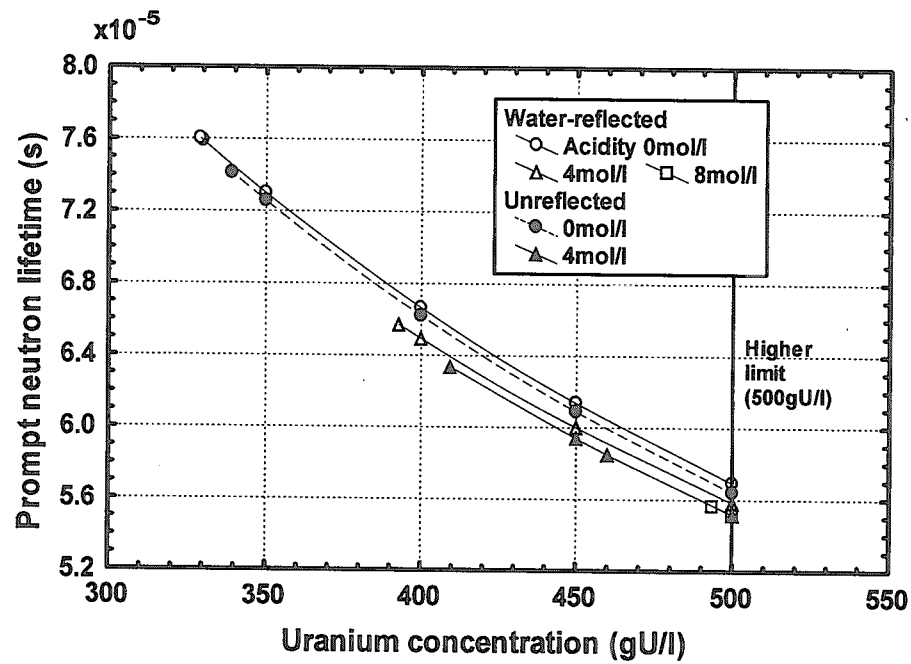


Figure 4.5.1 Prompt neutron lifetime without soluble neutron poison

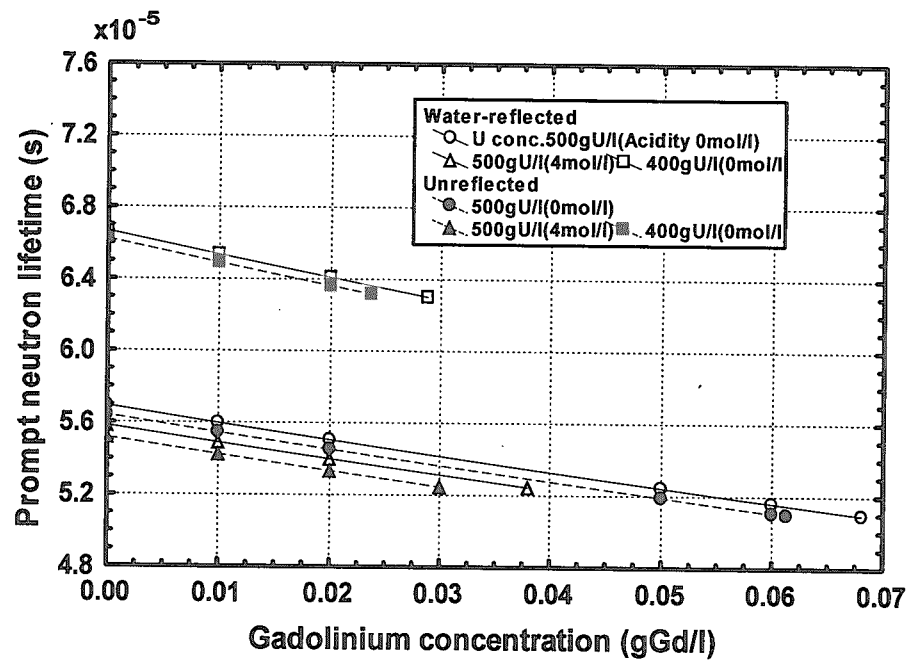


Figure 4.5.2 Prompt neutron lifetime with soluble neutron poison: gadolinium

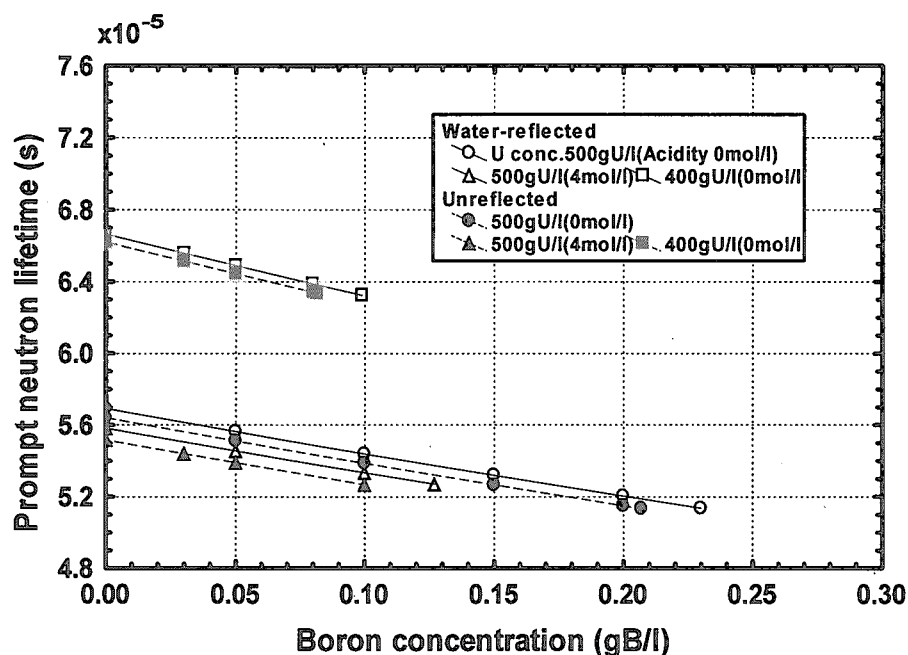


Figure 4.5.3 Prompt neutron lifetime with soluble neutron poison: boron

4.2 Excess Reactivity and Reactivity Addition Rate

The maximum excess reactivity is defined as the reactivity corresponding to a level of the higher electrodes of level meter (see Fig. 2.3), as mentioned in Chap.2. According to the definition, the maximum excess reactivity (ρ_{ex}) can be evaluated by,

$$\rho_{ex} = \frac{d\rho}{dh} \left(\frac{0.17}{\frac{d\rho}{dh}} + Z_e + Z_m \right), \dots \dots \dots (4.2.1)$$

$$= 0.17 + \frac{d\rho}{dh} (Z_e + Z_m)$$

where $d\rho/dh$, Z_e and Z_m represent differential reactivity of solution level height in the unit of $\$/mm$, distance between the lower and higher electrodes (1.8mm) and maximum incremental level (0.5mm) due to time delay in stoppage of the solution feed after the level detection by the higher electrodes, respectively. For the

maximum incremental level, we assumed that there was one-second delay in the stoppage of the solution feed while the incremental speed of level was set to be 0.5mm/s as its maximum. From Eq.(4.2.1), the maximum excess reactivity obviously increases as the differential reactivity of solution level height increases. Consequently, the maximum excess reactivity is evaluated to be 0.34\$ by using the maximum differential reactivity of solution level height, 0.072\$/mm, confirmed in Sec.4.1. The evaluated value, therefore, complies with the criterion (within 0.8\$) sufficiently.

The reactivity addition rate at the vicinity of the critical level height ($d\rho/dt$) is expressed by,

$$\frac{d\rho}{dt} = \frac{d\rho}{dh} \cdot \frac{W}{60} \frac{10000}{\pi \left(\frac{D}{2}\right)^2}, \dots\dots\dots (4.2.2)$$

where W and D represent a flow rate by the slow pump in the unit of l/min and an inner diameter of the core tank (79cm), respectively. The slow pump can control a flow rate in the range of 0.7 to 10l/min, as described in Chap.2, which is manually adjusted prior to the operation. Using Eq.(4.2.2), the flow rate corresponding to the maximum reactivity addition rate (3cent/s) is evaluated to be 12l/min in the case of the maximum differential reactivity of solution level height, 0.072\$/mm. The maximum flow rate of the slow pump is sufficiently smaller than the evaluated flow rate corresponding to the rate of 3 cent/s. For this reason, it is confirmed that the slow pump satisfies the required condition to control reactivity addition rates within 3cent/s.

4.3 Reactivity Effect by Free Surface Sloshing

Figure 4.6 shows typical results of reactivity effects brought by free surface sloshing. It is confirmed from Fig.4.6 that the negative reactivity is added by the sloshing. According to the study by Miyoshi *et al.*,⁸⁾ the reactivity effect by the sloshing is always negative on condition that the minimum critical level height is 40cm for cylindrical cores having a diameter within 80cm. The sloshing effect depends mainly upon variation of neutron leakage toward the vertical direction. For cores having small amounts of such neutron leakage, *i.e.* a high solution level, the reactivity effect becomes small. For this reason, the negative reactivity decreases as the solution level height increases, as seen in Fig.4.6. Also, the larger

negative reactivity is found under the unreflected conditions compared with that under the water-reflected conditions. This is also due to the same reason.

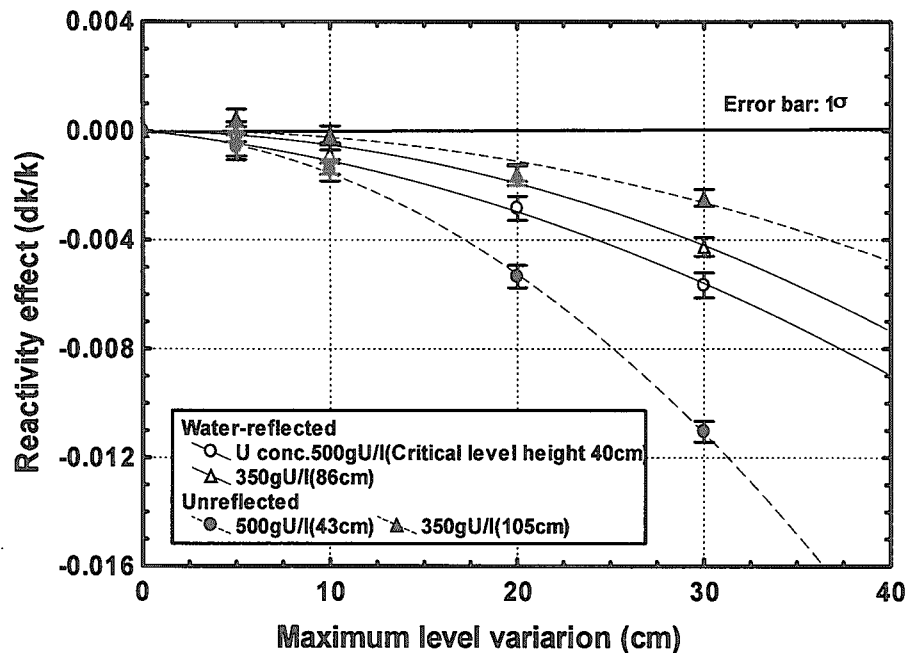


Figure 4.6 Reactivity effect caused by free surface sloshing

4.4 Shutdown Margin by Safety Rods

For the stationary surface of solution not containing soluble neutron poisons, Figs. 4.7.1(1) and 4.7.1(2) show the neutron multiplication factors in the cases of all safety rods inserted and one safety rod not inserted into the solution, respectively. Also, Figs. 4.7.2(1) to 4.7.3(2) show the neutron multiplication factors for cores containing gadolinium and boron. The plotted points in these figures are calculated values plus tripled standard deviations due to Monte Carlo technique. For all cases, the neutron multiplication factors (k_{eff}) were evaluated by,

$$k_{eff} = \frac{1}{1 - (\rho_{ex} + \rho_m) + \rho_{rod}}, \quad (4.4.1)$$

where ρ_{rod} , ρ_{ex} and ρ_m represent reactivity worth by safety rods, maximum excess

reactivity (0.8% multiplied by effective delayed neutron fraction) and a safety margin ($=0.5\%\Delta k/k$), respectively.

It is considered that the reactivity effect by safety rods basically depends on the following points,

- Neutron absorption rates of solution, increase of which will lead to the decrease of reactivity effect by safety rods,
- Neutron leakage from the core, decrease of which will lead to the decrease of reactivity effect.

In addition, geometrical conditions on the vertical position of safety rods in the core will greatly affect the reactivity effect. As illustrated in Fig.3.3.2, the neutron absorber (boron carbide) does not reach the bottom of core even if the safety rod is fully inserted into the core. This implies that the reactivity effect by safety rods will decrease relatively as the critical level height becomes smaller. As seen in Figs. 4.7.2(1) to 4.7.3(2), the neutron multiplication factors slightly decrease as the increase of concentration of soluble neutron poisons and free nitric acid, which lead to larger neutron absorption rates and to larger critical level heights. They provide larger neutron multiplication factors in terms of neutron absorption in the core and leakage from the core. The tendency of the neutron multiplication factors in Figs. 4.7.2(1) to 4.7.3(2) is, however, considered to be mainly due to the above-mentioned geometrical conditions of the inserted safety rods, which result in smaller neutron multiplication factors for larger critical level heights. In the case of cores not containing soluble neutron poisons, the neutron multiplication factors increase as the uranium concentration increases, as seen in Figs. 4.7.1(1) and 4.7.1(2), since such variation of the concentration will lead to larger neutron absorption rates and smaller critical level heights. For all cases, the neutron multiplication factors under water-reflected conditions are larger than those under unreflected conditions. This is because the effect of reflector brings smaller neutron leakage from the core as well as lower critical level heights. It is also confirmed that the neutron multiplication factors for all cases comply with the criteria mentioned in Chap.2 sufficiently. The shutdown margin by the safety rods under the stationary surface conditions becomes minimum under the following condition.

- Uranium concentration: 500gU/l.
- Concentration of free nitric acid: 0mol/l.
- Soluble neutron poison: none.
- Critical level height: 40.0cm.

- Reflector: water.

The free surface sloshing effects on the shutdown margin by safety rods were also confirmed under the condition of 500gU/l of uranium concentration and 0mol/l of free nitric acid concentration. The results are shown in Figs. 4.8(1) and 4.8(2). In the case of all safety rods inserted into the solution, the neutron multiplication factors do not greatly vary with the maximum level variation. It is considered that the decrease of safety rod worth due to the sloshing might be compensated by the negative reactivity effect brought by the sloshing shown in Fig.4.6. The neutron multiplication factors, however, increase significantly with the maximum level variation in the case of one safety rod not inserted into the core having the smallest critical level height. For small critical level heights, it is considered that the safety rod placed at the horizontally symmetrical position to the safety rod not inserted is not effective to add negative reactivity in the case of the sloshing surface, as illustrated in Fig.3.3.3. This leads to the condition that two rods are not inserted substantially. Even if the sloshing effect is taken into account, it is confirmed that the shutdown margin by the safety rods complies with the criteria sufficiently.

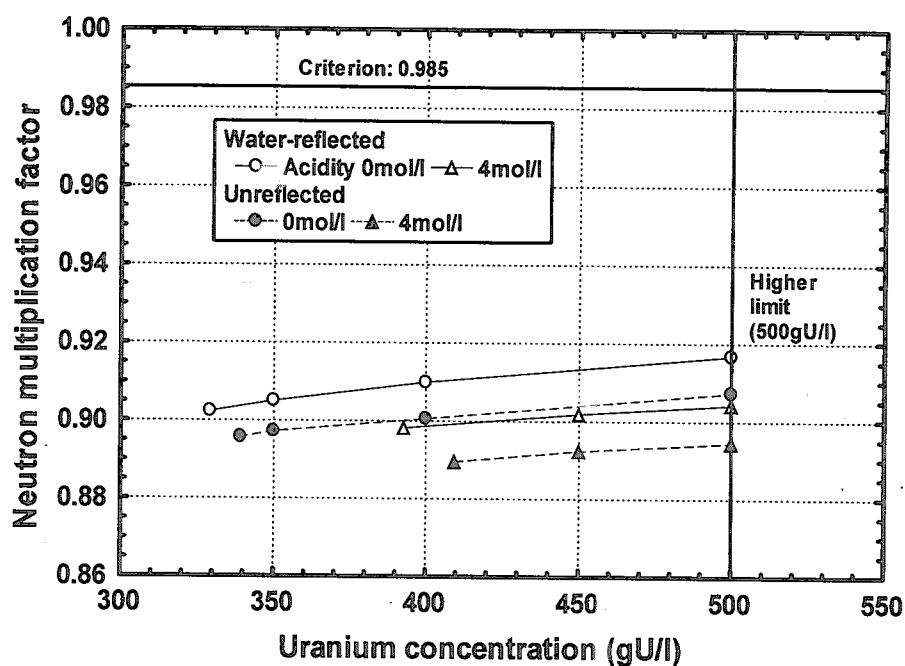


Figure 4.7.1(1) Neutron multiplication factor in case of all safety rods inserted into solution without soluble neutron, having stationary surface

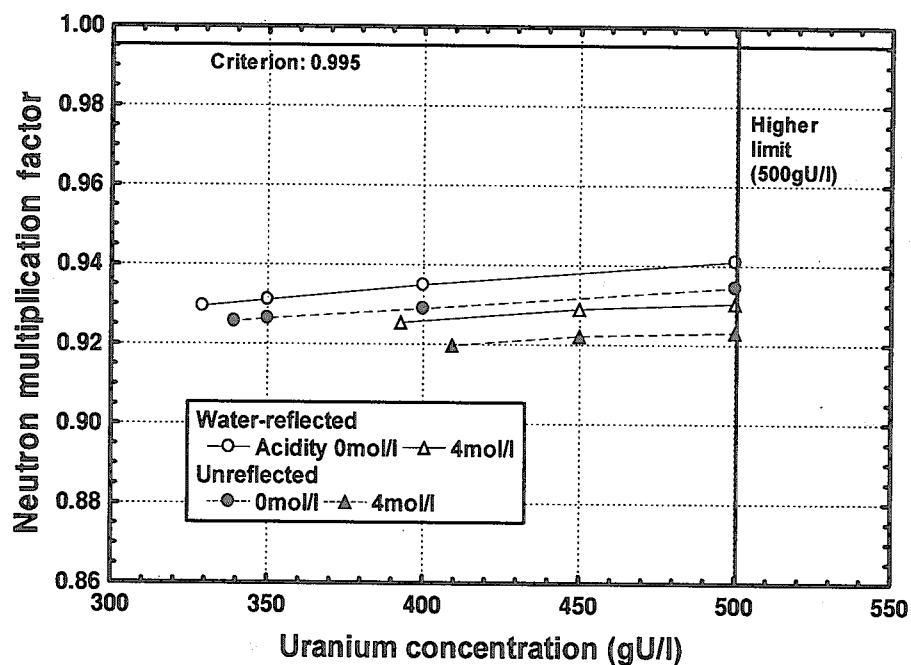


Figure 4.7.1(2) Neutron multiplication factor in case of one safety rod not inserted into solution without soluble neutron poison, having stationary surface

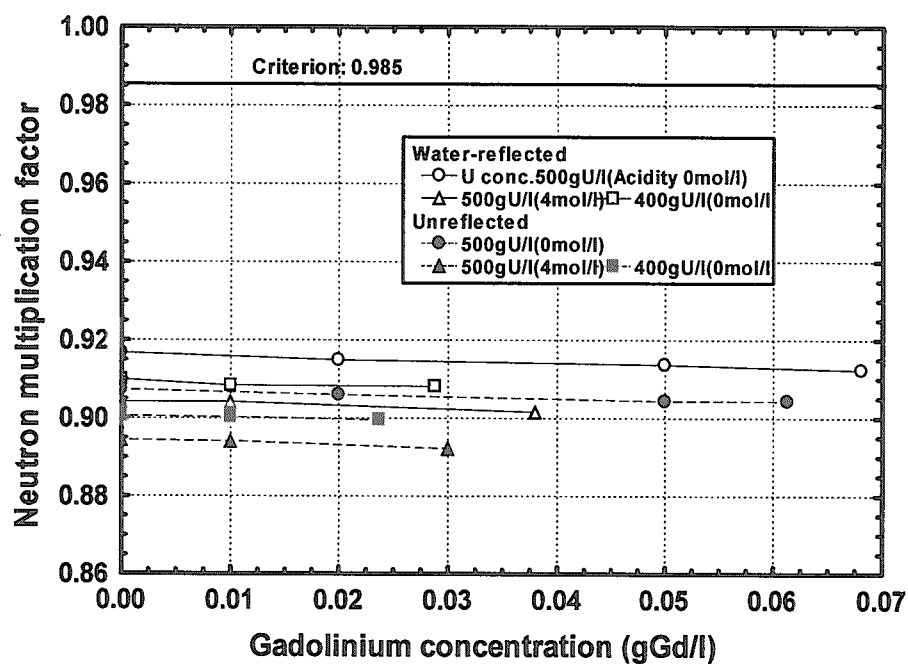


Figure 4.7.2(1) Neutron multiplication factor in case of all safety rods inserted into solution with soluble neutron poison: gadolinium, having stationary surface

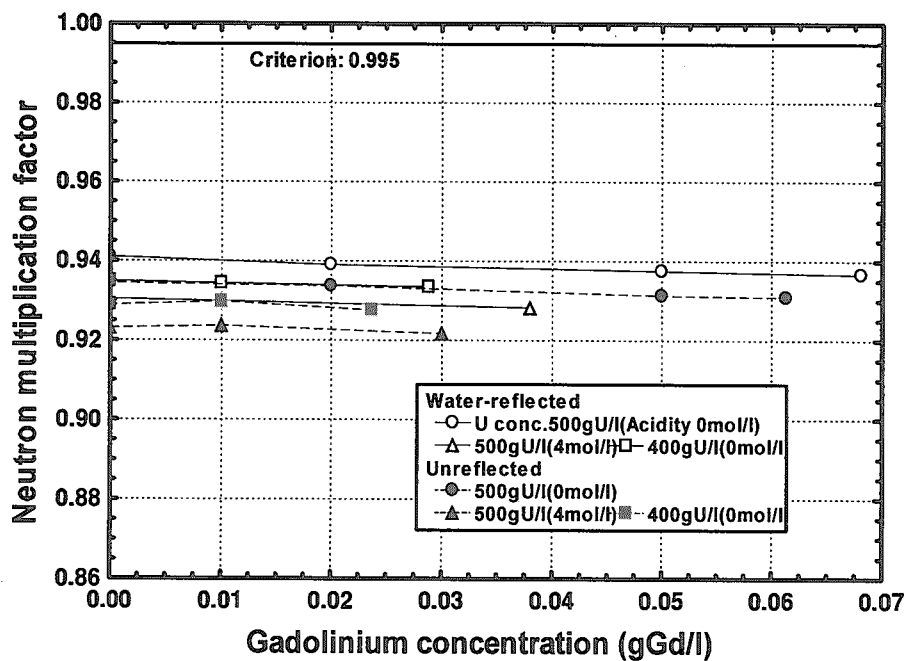


Figure 4.7.2(2) Neutron multiplication factor in case of one safety rod not inserted into solution with soluble neutron poison: gadolinium, having stationary surface

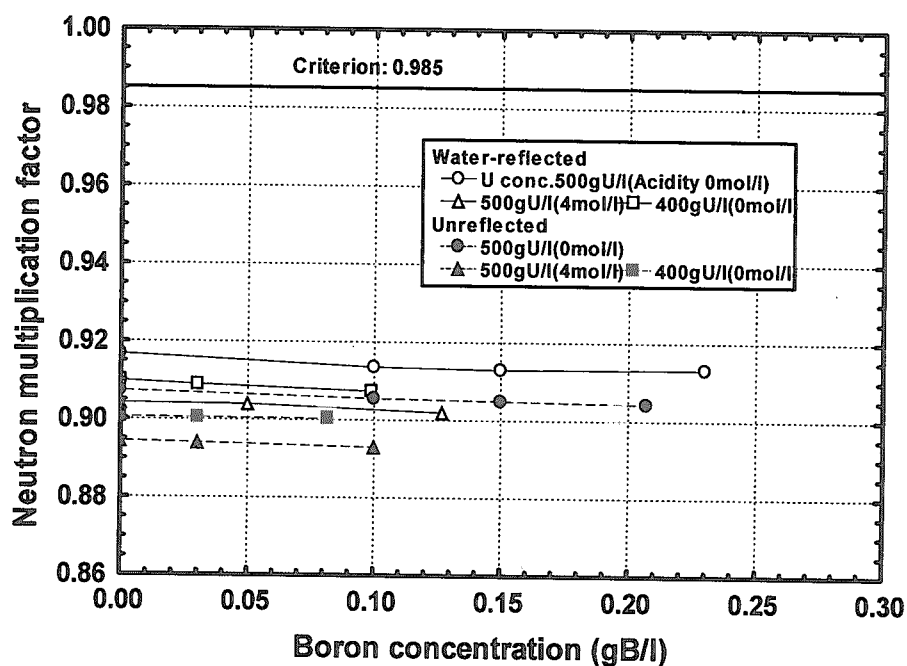


Figure 4.7.3(1) Neutron multiplication factor in case of all safety rods inserted into solution with soluble neutron poison: boron, having stationary surface

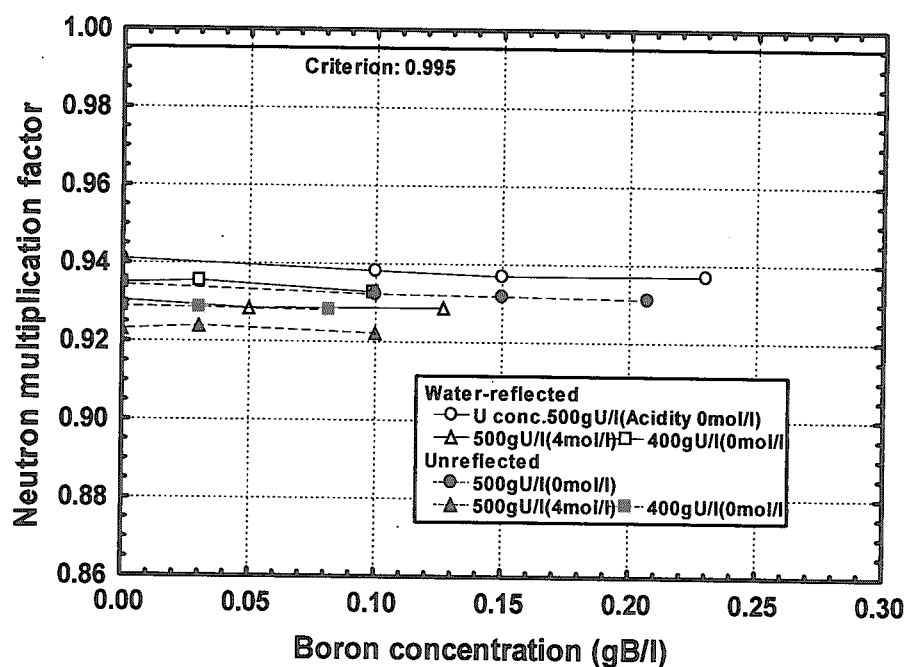


Figure 4.7.3(2) Neutron multiplication factor in case of one safety rod not inserted into solution with soluble neutron poison: boron, having stationary surface

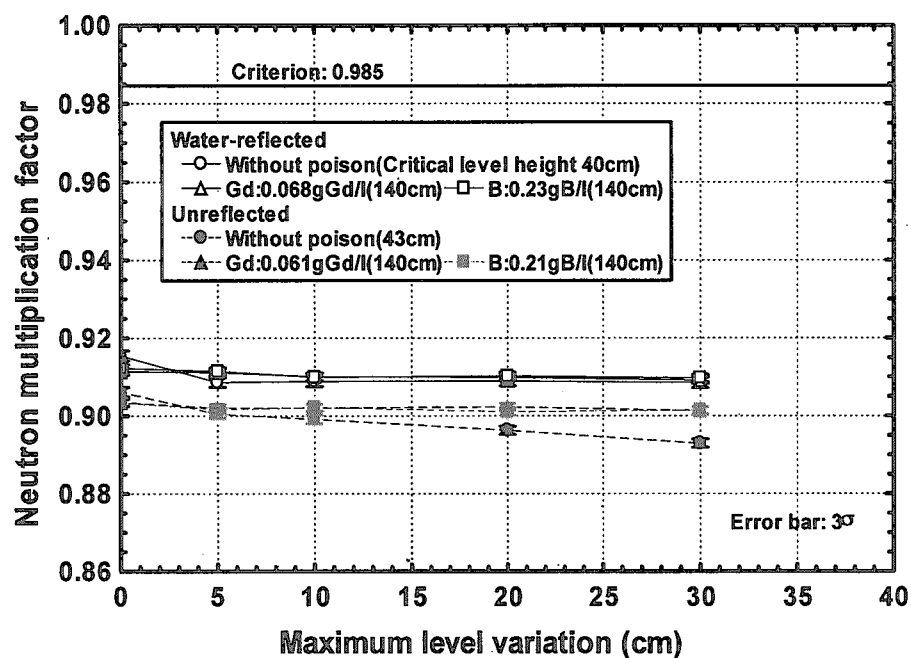


Figure 4.8(1) Neutron multiplication factor in case of all safety rods inserted into solution under sloshing condition (U conc. 500gU/l, Acidity 0mol/l)

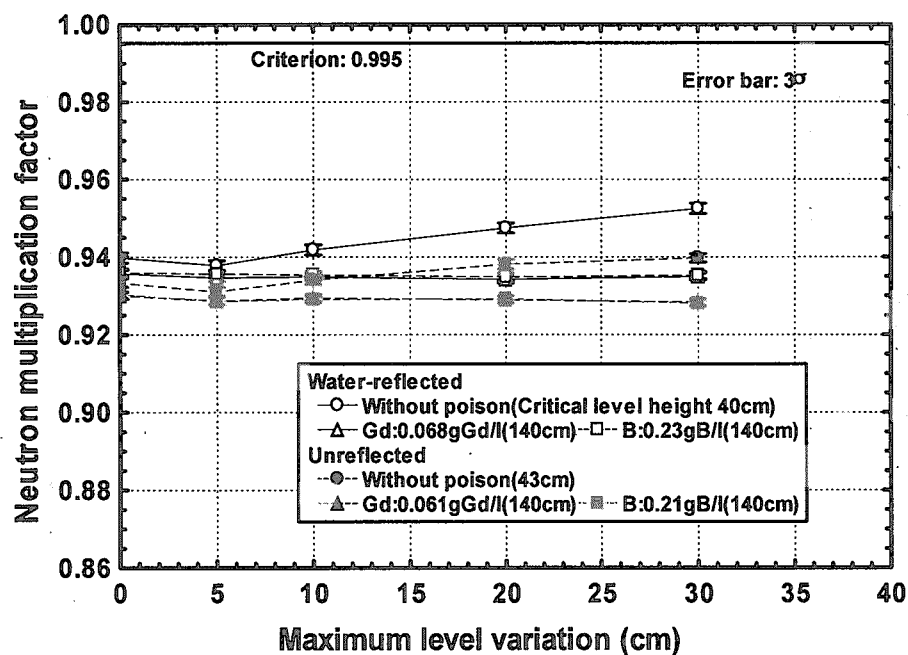


Figure 4.8(2) Neutron multiplication factor in case of one safety rod not inserted into solution under sloshing condition (U conc. 500gU/l, Acidity 0mol/l)

5. Summary and Conclusion

As a preliminary safety examination of the 80-cm-diameter cylindrical cores fueled with 6% enriched uranyl nitrate solution in STACY, neutronic characteristics of cores have been evaluated by the method of neutron diffusion and transportation calculations. First, critical level heights of cores were surveyed with such parameters as uranium concentration, concentration of free nitric acid, concentration of soluble neutron poison, gadolinium and boron. It has been confirmed from the evaluation that all critical cores comply with the safety criteria sufficiently concerning the excess reactivity, reactivity addition rates at the vicinity of a critical level height, and shutdown margins by safety rods, which are fundamental criteria for the STACY operations.

After the core is composed at STACY, the compliance with the safety criteria will be examined again by using operational and experimental data as well as computational results. These results will be also presented in the future.

Acknowledgement

The authors would like to thank Dr. T. Mori, Head of Research Group for Reactor Physics, JAERI, for his advice on the MVP calculations and helpful comments on the manuscript. Thanks are due to Mr. A. Ohno of the authors' Department for his helpful discussion on the work. The authors also would like to acknowledge encouragement and advice from Dr. Y. Suzuki, Director of the Department.

References

- 1) K. Murakami, S. Onodera, H. Hirose, *et al.*, *Construction of STACY (Static Experiment Critical Facility)*, JAERI-Tech 98-033, Japan Atomic Energy Research Institute (1998) [in Japanese].
- 2) Y. Miyoshi, T. Umamo, K. Tonoike, *et al.*, "Critical experiments on 10% enriched uranyl nitrate solution using a 60-cm-diameter cylindrical core," *Nucl. Technol.*, 118, 69 (1997).
- 3) S. Watanabe, Y. Yamane, Y. Miyoshi, *et al.*, *STACY: 80-cm-diameter cylindrical*

- tank of 10%-enriched uranyl nitrate solutions, water-reflected, LEU-SOL-THERM-020, NEA/NSC/DOC(95)03/IV, OECD/NEA (2002).*
- 4) S. Watanabe, Y. Yamane, Y. Miyoshi, *et al.*, *STACY: 80-cm-diameter cylindrical tank of 10%-enriched uranyl nitrate solutions, unreflected, LEU-SOL-THERM-021, NEA/NSC/DOC(95)03/IV, OECD/NEA (2002).*
 - 5) T. Yamamoto, Y. Miyoshi, T. Kikuchi, *et al.*, "Criticality safety benchmark experiment on 10% enriched uranyl nitrate solution using a 28-cm-thickness slab core," *J. Nucl. Sci. Technol.*, **39**[7], 789 (2002).
 - 6) K. Tonoike, Y. Miyoshi, T. Kikuchi, *et al.*, "Kinetic parameter β_{eff}/ℓ measurement on low enriched uranyl nitrate solution with single unit cores (600 ϕ , 280T, 800 ϕ) of STACY," *J. Nucl. Sci. Technol.*, **39**[11], 1227 (2002).
 - 7) T. Suzaki, Y. Miyoshi, "Measurements of reactivity effects caused by surface waves excited in nuclear fuel systems having a free surface," *J. Nucl. Sci. Technol.*, **23**[9], 840 (1986).
 - 8) Y. Miyoshi, H. Hirose, T. Suzaki, "Measurements and calculations on sloshing effects in solution vessels having a free surface," *Proc. Int. Seminar on Nuclear Criticality Safety (ISCS'87)*, p. 50, Oct. 19-23, 1987, Tokyo, Japan (1987).
 - 9) T. B. Fowler, D. R. Vondy, *Nuclear reactor core analysis code: CITATION*, ORNL-TM-2496, Oak Ridge National Laboratory (1969).
 - 10) K. Okumura, K. Kaneko, K. Tsuchihashi, *SRAC95: General purpose neutronics code system*, JAERI-Data/Code 96-015, Japan Atomic Energy Research Institute (1996) [in Japanese].
 - 11) K. Shibata, T. Kawano, T. Nakagawa, *et al.*, "Japanese evaluated nuclear data library version 3 revision-3: JENDL-3.3," *J. Nucl. Sci. Technol.*, **39**[11], 1125 (2002).
 - 12) S. Sakurai, S. Tachimori, "Density equation of aqueous solution containing plutonium (IV), uranium (VI) and nitric acid," *J. Nucl. Sci. Technol.*, **33**[2], 187 (1996).
 - 13) T. Mori, M. Nakagawa, M. Sasaki, "Vectorization of continuous energy Monte Carlo method for neutron transport calculation," *J. Nucl. Sci. Technol.*, **29**[4], 325 (1992).
 - 14) T. Mori, M. Nakagawa, *MVP/GMVP: General purpose Monte Carlo codes for neutron and photon transport calculations based on continuous energy and multigroup methods*, JAERI-Data/Code 94-007, Japan Atomic Energy Research Institute (1994) [in Japanese].
 - 15) N. Yasuda, I. Shichiji, K. Sakuraba, *et al.*, Private communication (1991).

- 16) Nuclear Safety Committee, Japan, *Guidelines for Safety Review on Seismic Design of Power Reactors*, July 20, 1981 [in Japanese].
- 17) K. D. Lathlop, F. W. Brinkly, *Theory and use of the general geometry TWOTRAN program*, LA-4432, Los Alamos National Laboratory (1970).
- 18) A. Tsiboulia, B. Riazanov, M. Nikolaev, *et al.*, *Uranium nitrate solution (70gU/l) with gadolinium*, HEU-SOL-THERM-014, NEA/NSC/DOC(95)03/II, OECD/NEA (2002).
- 19) A. Tsiboulia, B. Riazanov, M. Nikolaev, *et al.*, *Uranium nitrate solution (100gU/l) with gadolinium*, HEU-SOL-THERM-015, NEA/NSC/DOC(95)03/II, OECD/NEA (2002).
- 20) A. Tsiboulia, B. Riazanov, M. Nikolaev, *et al.*, *Uranium nitrate solution (150gU/l) with gadolinium*, HEU-SOL-THERM-014, NEA/NSC/DOC(95)03/II, OECD/NEA (2002).
- 21) A. Tsiboulia, B. Riazanov, M. Nikolaev, *et al.*, *Uranium nitrate solution (200gU/l) with gadolinium*, HEU-SOL-THERM-014, NEA/NSC/DOC(95)03/II, OECD/NEA (2002).
- 22) A. Tsiboulia, B. Riazanov, M. Nikolaev, *et al.*, *Uranium nitrate solution (300gU/l) with gadolinium*, HEU-SOL-THERM-014, NEA/NSC/DOC(95)03/II, OECD/NEA (2002).
- 23) A. Tsiboulia, B. Riazanov, M. Nikolaev, *et al.*, *Uranium nitrate solution (400gU/l) with gadolinium*, HEU-SOL-THERM-014, NEA/NSC/DOC(95)03/II, OECD/NEA (2002).
- 24) A. Tsiboulia, Y. Rozhikhin, V. Gurin, *et al.*, *Boron carbide absorber rods in uranium (5.64% ^{235}U) nitrate solution*, LEU-SOL-THERM-005, NEA/NSC/DOC(95)03/IV, OECD/NEA (2002).
- 25) A. Tsiboulia, Y. Rozhikhin, V. Gurin, *et al.*, *Boron carbide absorber rods in uranium (10% ^{235}U) nitrate solution*, LEU-SOL-THERM-005, NEA/NSC/DOC(95)03/IV, OECD/NEA (2002).

Appendix-1 Reactivity Effects by Temperature Variation

The reactivity effects brought by temperature variation up to 40°C, which is the maximum temperature of the STACY cores, were evaluated by using the CITATION code in the SRAC code system. Figures A.1.1, A.1.2 and A.1.3 show results of the reactivity effects. For homogeneous uranium solution systems, the reactivity variation by temperature increase is considered to be mainly due to the decrease of solution density, which leads to the increase of neutron leakage and harder neutron energy spectrum. For this reason, the reactivity is negative. In the case of unreflected conditions, the negative reactivity is slightly larger than that under water-reflected conditions. This is because the neutron leakage under unreflected conditions is larger than that under water-reflected ones.

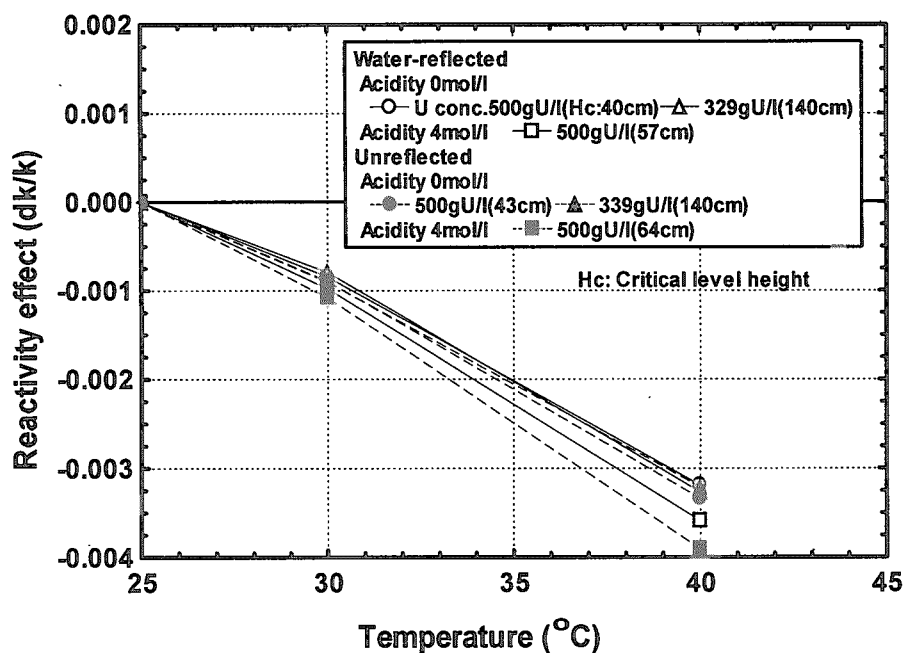


Figure A.1.1 Reactivity effect by temperature variation of solution without soluble neutron poison

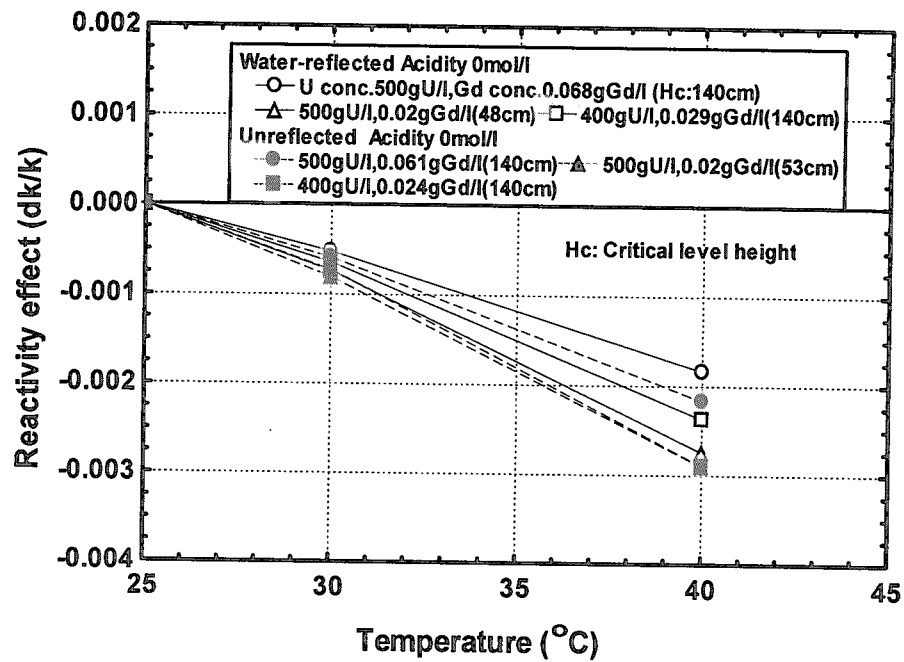


Figure A.1.2 Reactivity effect by temperature variation of solution with soluble neutron poison: gadolinium

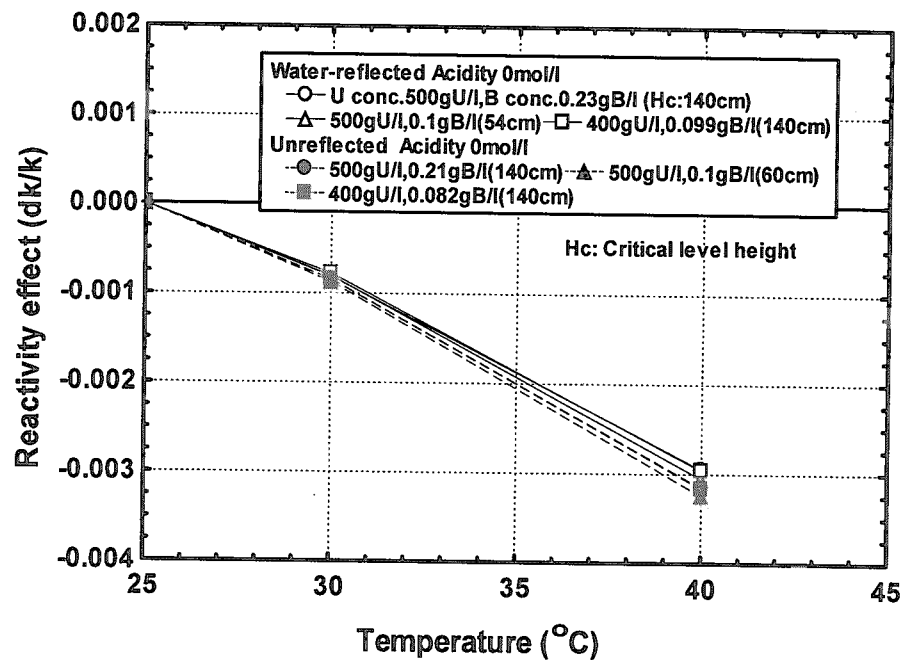


Figure A.1.3 Reactivity effect by temperature variation of solution with soluble neutron poison: boron

Appendix-2 Validation of Calculation Method

The validity of the calculation methods has been confirmed by benchmark calculations on published experimental data, of which conditions are similar to the present core configurations. The results of benchmark tests are described below.

(1) Criticality

STACY experiments using low-enriched uranyl nitrate solution

The 80-cm-diameter core tank had been used in STACY with 10% enriched uranyl nitrate solution containing no soluble neutron poison. The results were published as benchmark problems in the International Criticality Safety Benchmark Evaluation Project (ICSBEP) handbook.^{3,4)} For these benchmark problems, the validity of the present calculation methods was confirmed. As reference, two-dimensional neutron transport calculations (P_1S_8) were also performed using the TWOTRAN¹⁷⁾ code in the SRAC code system.

Table A.2.1 lists the results of benchmark tests. For the CITATION code, the biases of neutron multiplication factor (k_{eff}) are confirmed to be in the range of -1 to -0.3%. The biases of k_{eff} by the MVP code are much smaller than those by the CITATION code, which are in the range of -0.2 to +0.1%. The discrepancies of k_{eff} between the CITATION and TWOTRAN codes are 1.3% in maximum. It is confirmed that these computational codes well reproduce the experimental results.

Table A.2.1 Results of benchmark tests on neutron multiplication factors of STACY 80-cm-diameter cylindrical cores fueled with 10% enriched uranyl nitrate solution

Run ^{a)}	Ref-lector	Experimental k_{eff}	SRAC-CITATION		SRAC-TWOTRAN		MVP	
			k_{eff}	C/E	k_{eff}	C/E	k_{eff}	C/E
216	Water	0.9995 ± 0.0010	0.9900	0.9905	1.0029	1.0034	1.0004 ± 0.0003	1.0009
217		0.9996 ± 0.0010	0.9917	0.9921	1.0033	1.0037	0.9998 ± 0.0003	1.0002
220		0.9997 ± 0.0012	0.9935	0.9938	1.0033	1.0036	0.9989 ± 0.0002	0.9992
226		0.9998 ± 0.0012	0.9959	0.9961	1.0045	1.0047	0.9998 ± 0.0002	1.0000
215	None	0.9983 ± 0.0009	0.9883	0.9900	0.9999	1.0016	0.9959 ± 0.0003	0.9976
218		0.9985 ± 0.0010	0.9909	0.9924	1.0013	1.0028	0.9972 ± 0.0003	0.9987
221		0.9989 ± 0.0011	0.9927	0.9938	1.0013	1.0024	0.9968 ± 0.0002	0.9979
223		0.9993 ± 0.0012	0.9959	0.9966	1.0033	1.0040	0.9988 ± 0.0002	0.9995

a) See Refs. 3 and 4.

The comparisons of the differential reactivity of solution level height (dp/dh) between the CITATION and TWOTRAN codes on 80-cm-diameter cylindrical cores fueled with 6% enriched uranyl nitrate solution are also listed in Table A.2.2, aiming at water-reflected and unreflected cores having the smallest critical level height. As described in Chap.4, the smallest critical level height leads to the largest differential reactivity, which is used for the evaluation of the maximum excess reactivity and reactivity addition rates. The CITATION code provides about 6% larger differential reactivity in comparison with the TWOTRAN code and more conservative results than those by the TWOTRAN code, as listed in Table A.2.2.

Table A.2.2 Comparisons of differential reactivity of solution level height between CITATION and TWOTRAN codes on STACY 80-cm-diameter cylindrical cores fueled with 6% enriched uranyl nitrate solution (U conc. 500gU/l, acidity 0mol/l, without soluble neutron poisons)

Ref-lector	Level height (cm)	SRAC-CITATION	SRAC-TWOTRAN	CITATION / TWOTRAN
		dp/dh (% $\Delta k/k$)	dp/dh (% $\Delta k/k$)	
Water	40.04	0.052	0.049	1.064
None	42.97	0.046	0.043	1.056

IPPE experiments using highly enriched uranyl nitrate solution containing gadolinium

For low-enriched uranyl nitrate solution containing soluble neutron poisons, no benchmark data is currently available in the ICSBEP handbook. The handbook covers experimental data on 89.04% enriched uranyl nitrate solution containing gadolinium obtained by the Institute of Physics and Power Engineering (IPPE), Russia.¹⁸⁻²³⁾ The experiments were carried out by using a 40-cm-diameter cylindrical core tank with water reflector. The uranium concentration was in the range of 70 to 400gU/l. The uranium-235 concentration was 62g²³⁵U/l for the solution of 70gU/l, which is the closest to that of STACY with 6% enriched uranyl nitrate solution (max. 30g²³⁵U/l). Therefore, the benchmark calculations were performed on the solution of 70gU/l¹⁸⁾ using CITATION, TWOTRAN and MVP codes.

Table A.2.3 lists the results of the benchmark tests. It is found from the CITATION calculations on the cases 1 and 2 that the discrepancies in k_{eff} are larger than that of 10% enriched uranium of STACY listed in Table A.2.1. This is considered to be due to fairly small critical level heights for these cases. For the

cases 2 and 3, larger discrepancies in k_{eff} are also found in the MVP and TWOTRAN calculations. Similar discrepancies are confirmed even though the different Monte Carlo codes and nuclear data libraries are used.¹⁸⁾ Figure A.2.1 shows ratios of the calculated k_{eff} . The ratios of k_{eff} of the CITATION code to the MVP code tend to decrease significantly as the critical level heights decrease. This tendency is also found in the ratios of k_{eff} of the TWOTRAN code to the MVP code, but their variation is much smaller than that of the ratios of k_{eff} of the CITATION code to the MVP code. This implies that the neutron-diffusion technique might not be applicable to the systems having small critical level heights like the IPPE cases 1 and 2. The IPPE experimental cores had water reflector under the core tank as well as the same reflector for the horizontal direction. On the solution core, however, no reflector existed. This configuration is similar to STACY. In particular, the Fick's law is considered to be not applicable to a region at the vicinity of the unreflected top boundary. In the case of smaller core heights presented in the IPPE cases 1 and 2, this region becomes relatively greater in the whole of core.

Figures A.2.2 and A.2.3 show calculated neutron energy spectra on the IPPE case 1 and 3 experiments, respectively. For both cases, the neutron spectra at the center of core by the CITATION code well agree with those by the TWOTRAN code. On the other hand, it is clarified from the results of case 1 that the neutron spectrum at the vicinity of the top boundary by the CITATION code is harder than that by the TWOTRAN code. For this reason, k_{eff} by the CITATION code is smaller than that by the TWOTRAN code, as listed in Table A.2.3. For the case 3, the discrepancy of the spectra at the vicinity of the boundary is reduced, as shown in Fig. A.2.3(b).

The minimum critical level height is, however, 40cm in STACY. Besides, the CITATION code well reproduces the IPPE case 3 (45cm of critical level height), as listed in Table A.2.3. The neutron-diffusion technique is, therefore, considered to be applicable to the STACY systems as useful approximation.

Table A.2.3 Results of benchmark tests on neutron multiplication factors of uranyl nitrate solution systems (70gU/l) containing gadolinium

Case ^{a)}	Experimental k_{eff}	SRAC-CITATION		SRAC-TWOTRAN		MVP	
		k_{eff}	C/E	k_{eff}	C/E	k_{eff}	C/E
1	1.0000 ± 0.0028	0.9519	0.9519	0.9865	0.9865	0.9947 ± 0.0004	0.9947
2	1.0000 ± 0.0052	0.9811	0.9811	1.0103	1.0103	1.0115 ± 0.0004	1.0115
3	1.0000 ± 0.0087	1.0016	1.0016	1.0256	1.0256	1.0205 ± 0.0003	1.0205

a) See Ref. 18.

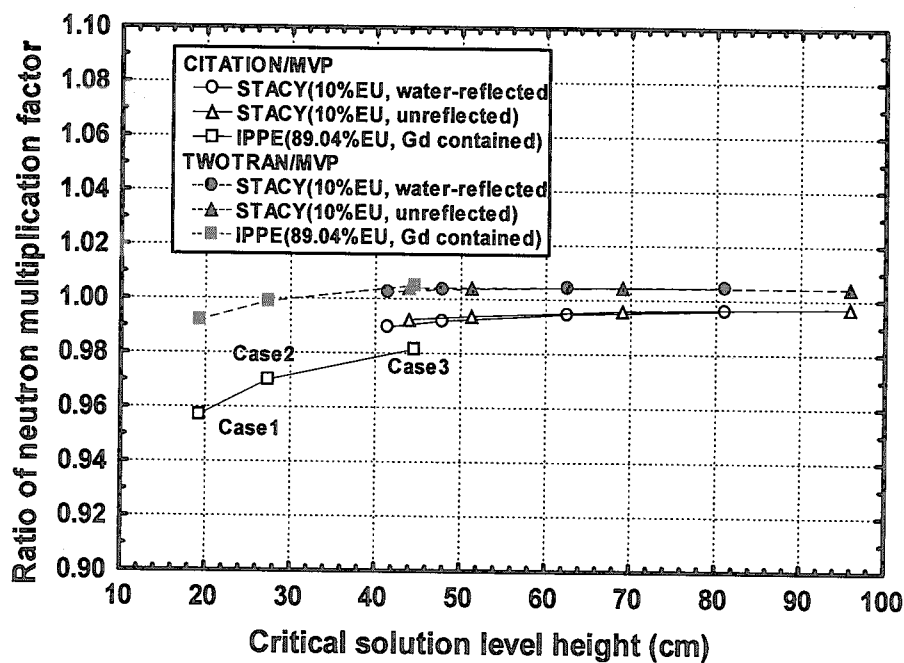
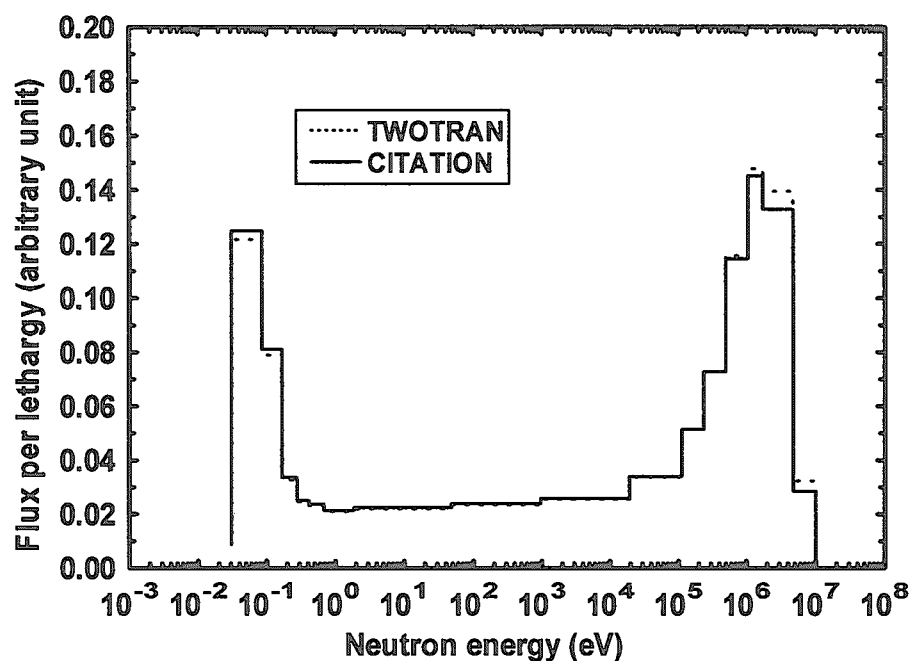
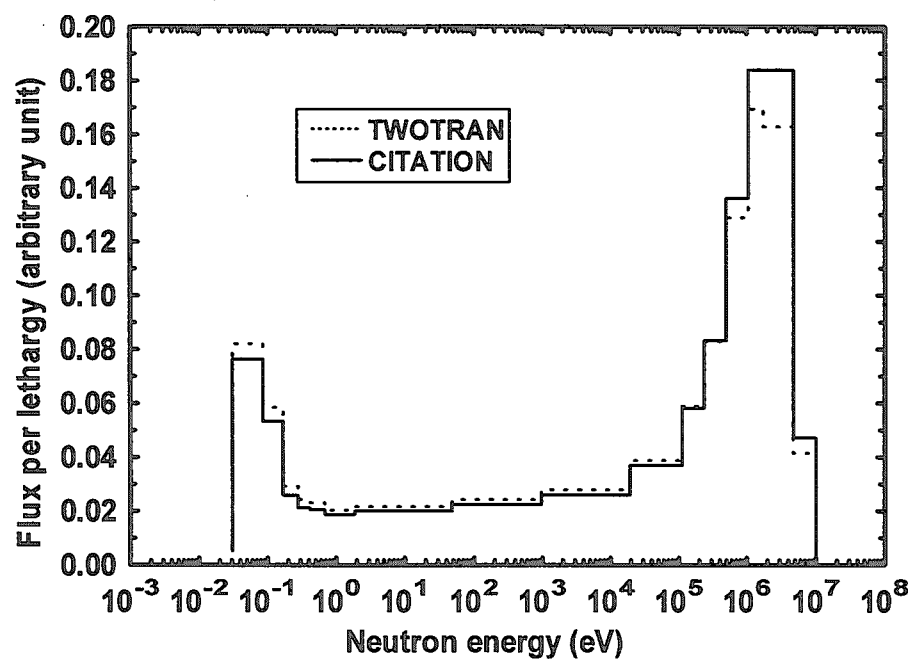


Figure A.2.1 Ratio of calculated neutron multiplication factor

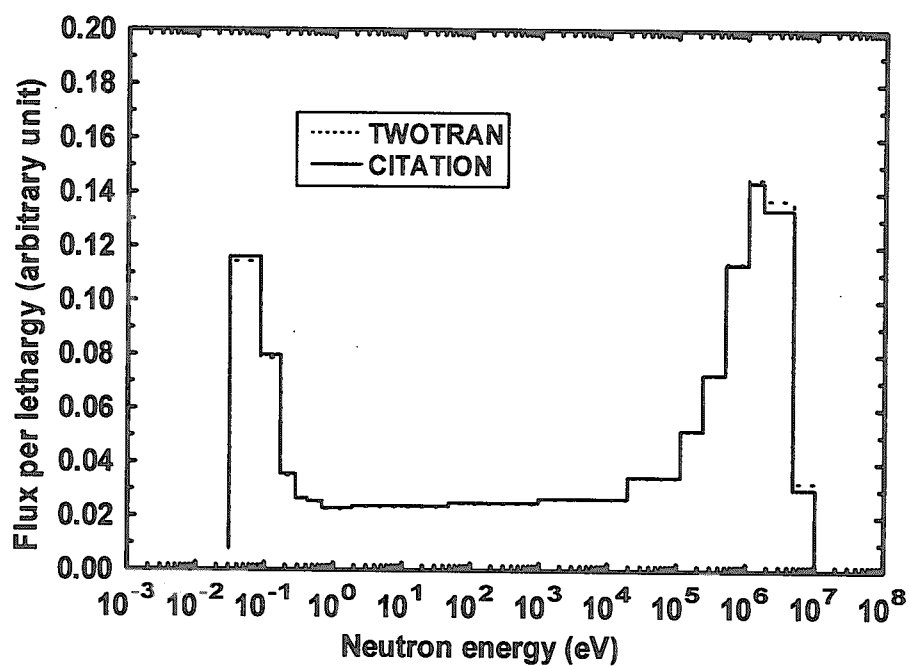


(a) Center of core

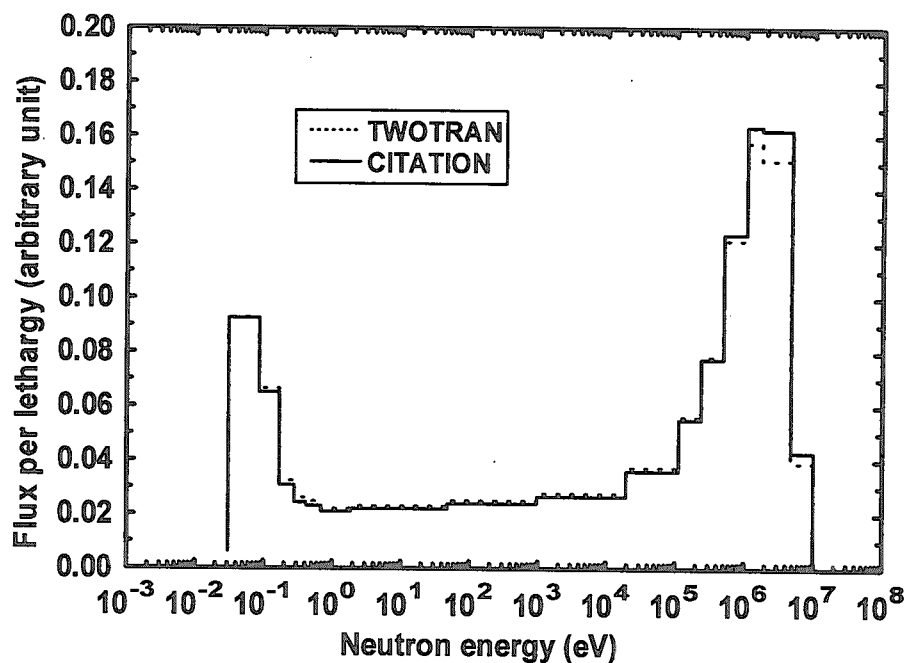


(b) Vicinity of top boundary (1/20 of core height inward from top boundary)

Figure A.2.2 Neutron energy spectra of IPPE Case 1 experiment using uranyl nitrate solution (70gU/l) containing gadolinium



(a) Center of core



(b) Vicinity of top boundary (1/20 of core height inward from top boundary)

Figure A.2.3 Neutron energy spectra of IPPE Case 3 experiment using uranyl nitrate solution (70gU/l) containing gadolinium

IPPE experiments using low-enriched uranyl nitrate solution containing absorber rods

In addition, benchmark tests on low- enriched uranyl nitrate solution systems containing boron carbide absorber rods were performed to confirm the validity of the calculations of safety rod worth. The benchmark problems are based on the criticality experiments carried out at IPPE.^{24,25)} In the experiments, absorber rods (5.5cm of outer diameter) were inserted into 5.64% or 10% enriched uranyl nitrate solution cores with water-reflector. The benchmark tests were performed by using the MVP code. Table A.2.4 lists the results of benchmark tests. The biases of k_{eff} by the MVP code are confirmed to be sufficiently small in the range of -0.1 to +0.7%, compared with the uncertainties in the experimental k_{eff} .

Table A.2.4 Results of benchmark tests on neutron multiplication factors of uranyl nitrate solution systems containing boron carbide absorber rods

Case ^{a)}	²³⁵ U (%)	Experimental k_{eff}	MVP	
			k_{eff}	C/E
1	5.64	1.0000 ± 0.0042	0.9990 ± 0.0003	0.9990
2		1.0000 ± 0.0051	0.9993 ± 0.0003	0.9993
3		1.0000 ± 0.0064	1.0001 ± 0.0003	1.0001
1	10	1.0000 ± 0.0037	0.9998 ± 0.0004	0.9998
2		1.0000 ± 0.0038	1.0056 ± 0.0003	1.0056
3		1.0000 ± 0.0041	0.9999 ± 0.0004	0.9999
4		1.0000 ± 0.0041	1.0007 ± 0.0004	1.0007
5		1.0000 ± 0.0047	1.0066 ± 0.0003	1.0066

a) See Refs. 24 and 25.

(2) Kinetic parameter (β_{eff}/ℓ)

STACY experiments using low-enriched uranyl nitrate solution

For kinetic parameters involving β_{eff} which is used for reactivity in the unit of β , benchmark calculations using the CITATION code were performed on the STACY 80-cm-diameter cores with 10% enriched uranyl nitrate solution under unreflected conditions.⁶⁾ Table A.2.5 lists the results of benchmark tests. The biases of β_{eff}/ℓ are confirmed to be in the range of -1.8 to -0.6%, of which range is almost the same as reported.⁶⁾

Table A.2.5 Results of benchmark tests on kinetic parameters (β_{eff}/ℓ) of STACY 80-cm-diameter cylindrical cores fueled with 10% enriched uranyl nitrate solution

Run ^{a)}	Experimental β_{eff}/ℓ (s ⁻¹)	SRAC-CITATION	
		β_{eff}/ℓ (s ⁻¹)	C/E
215	109.2±1.8	107.8	0.9873
219	102.7±1.6	101.4	0.9878
222	95.4±1.7	93.6	0.9815
224	90.0±2.2	89.4	0.9935

a) See Ref. 6.

This is a blank page.

国際単位系 (SI) と換算表

表1 SI基本単位および補助単位

量	名称	記号
長さ	メートル	m
質量	キログラム	kg
時間	秒	s
電流	アンペア	A
熱力学温度	ケルビン	K
物質の量	モル	mol
光度	カンデラ	cd
平面角	ラジアン	rad
立体角	ステラジアン	sr

表3 固有の名称をもつSI組立単位

量	名称	記号	他のSI単位 による表現
周波数	ヘルツ	Hz	s ⁻¹
力	ニュートン	N	m·kg/s ²
圧力, 応力	パスカル	Pa	N/m ²
エネルギー, 仕事, 熱量	ジュール	J	N·m
工率, 放射束	ワット	W	J/s
電気量, 電荷	クーロン	C	A·s
電位, 電圧, 起電力	ボルト	V	W/A
静電容量	ファラド	F	C/V
電気抵抗	オーム	Ω	V/A
コンダクタンス	ジーメンズ	S	A/V
磁束	ウェーバ	Wb	V·s
磁束密度	テスラ	T	Wb/m ²
インダクタンス	ヘンリー	H	Wb/A
セルシウス温度	セルシウス度	°C	
光束	ルーメン	lm	cd·sr
照度	ルクス	lx	lm/m ²
放射能	ベクレル	Bq	s ⁻¹
吸収線量	グレイ	Gy	J/kg
線量等量	シーベルト	Sv	J/kg

表2 SIと併用される単位

名称	記号
分, 時, 日	min, h, d
度, 分, 秒	°, ', "
リットル	l, L
トン	t
電子ボルト	eV
原子質量単位	u

1 eV=1.60218×10⁻¹⁹J
1 u=1.66054×10⁻²⁷kg

表5 SI接頭語

倍数	接頭語	記号
10 ¹⁸	エクサ	E
10 ¹⁵	ペタ	P
10 ¹²	テラ	T
10 ⁹	ギガ	G
10 ⁶	メガ	M
10 ³	キロ	k
10 ²	ヘクト	h
10 ¹	デカ	da
10 ⁻¹	デシ	d
10 ⁻²	センチ	c
10 ⁻³	ミリ	m
10 ⁻⁶	マイクロ	μ
10 ⁻⁹	ナノ	n
10 ⁻¹²	ピコ	p
10 ⁻¹⁵	フェムト	f
10 ⁻¹⁸	アト	a

表4 SIと共に暫定的に維持される単位

名称	記号
オングストローム	Å
バーン	b
バル	bar
ガリ	Gal
キュリー	Ci
レントゲン	R
ラド	rad
レム	rem

1 Å=0.1nm=10⁻¹⁰m
1 b=100fm²=10⁻²⁸m²
1 bar=0.1MPa=10⁵Pa
1 Gal=1cm/s²=10⁻²m/s²
1 Ci=3.7×10¹⁰Bq
1 R=2.58×10⁻⁴C/kg
1 rad=1cGy=10⁻²Gy
1 rem=1cSv=10⁻²Sv

(注)

- 表1-5は「国際単位系」第5版, 国際度量衡局 1985年刊行による。ただし, 1 eV および 1 u の値はCODATAの1986年推奨値によった。
- 表4には海里, ノット, アール, ヘクトールも含まれているが日常の単位なのでここでは省略した。
- bar は, JIS では流体の圧力を表す場合に限り表2のカテゴリに分類されている。
- E C 閣僚理事会指令では bar, barn および「血圧の単位」mmHgを表2のカテゴリに入れている。

換算表

力	N(=10 ⁵ dyn)	kgf	lbf
	1	0.101972	0.224809
	9.80665	1	2.20462
	4.44822	0.453592	1

粘度 1 Pa·s(N·s/m²)=10 P(ポアズ)(g/(cm·s))

動粘度 1 m²/s=10⁶St(ストークス)(cm²/s)

圧力	MPa(=10bar)	kgf/cm ²	atm	mmHg(Torr)	lbf/in ² (psi)
	1	10.1972	9.86923	7.50062×10 ³	145.038
	0.0980665	1	0.967841	735.559	14.2233
	0.101325	1.03323	1	760	14.6959
	1.33322×10 ⁻⁴	1.35951×10 ⁻³	1.31579×10 ⁻³	1	1.93368×10 ⁻²
	6.89476×10 ⁻³	7.03070×10 ⁻²	6.80460×10 ⁻²	51.7149	1

エネルギー・仕事・熱量	J(=10 ⁷ erg)	kgf·m	kW·h	cal(計量法)	Btu	ft·lbf	eV
	1	0.101972	2.77778×10 ⁻⁷	0.238889	9.47813×10 ⁻⁴	0.737562	6.24150×10 ¹⁸
	9.80665	1	2.72407×10 ⁻⁶	2.34270	9.29487×10 ⁻³	7.23301	6.12082×10 ¹⁹
	3.6×10 ⁶	3.67098×10 ⁵	1	8.59999×10 ⁵	3412.13	2.65522×10 ⁶	2.24694×10 ²⁵
	4.18605	0.426858	1.16279×10 ⁻⁶	1	3.96759×10 ⁻³	3.08747	2.61272×10 ¹⁹
	1055.06	107.586	2.93072×10 ⁻⁴	252.042	1	778.172	6.58515×10 ²¹
	1.35582	0.138255	3.76616×10 ⁻⁷	0.323890	1.28506×10 ⁻³	1	8.46233×10 ¹⁸
	1.60218×10 ⁻¹⁹	1.63377×10 ⁻²⁰	4.45050×10 ⁻²⁶	3.82743×10 ⁻²⁰	1.51857×10 ⁻²²	1.18171×10 ⁻¹⁹	1

1 cal= 4.18605J (計量法)
= 4.184J (熱化学)
= 4.1855J (15℃)
= 4.1868J (国際蒸気表)
仕事率 1 PS(仏馬力)
= 75 kgf·m/s
= 735.499W

放射能	Bq	Ci
	1	2.70270×10 ⁻¹¹
	3.7×10 ¹⁰	1

吸収線量	Gy	rad
	1	100
	0.01	1

照射線量	C/kg	R
	1	3876
	2.58×10 ⁻⁴	1

線量当量	Sv	rem
	1	100
	0.01	1

Evaluation of Neutronic Characteristics of STACY 80-cm-diameter Cylindrical Core Fueled with 6% Enriched Uranyl Nitrate Solution